


# Two galacturonosyltransferases function in plant growth, stomatal development, and dynamics

Huimin Guo,<sup>1</sup> Chuanlei Xiao,<sup>1</sup> Qing Liu,<sup>1</sup> Ruiying Li,<sup>1</sup> Zhiqiang Yan,<sup>1</sup> Xuan Yao<sup>2</sup> and Honghong Hu <sup>1,\*†</sup>

- 1 National Key Laboratory of Crop Genetic Improvement, College of Life Science and Technology, Huazhong Agricultural University, Wuhan 430070, China
- 2 College of Plant Science and Technology, Huazhong Agricultural University, Wuhan 430070, China

\*Author for communication: huhh@mail.hzau.edu.cn

†Senior author

H.H. conceived and designed the research. H.G., C.X., Q.L., R.L., and Z.Y. performed the experiments. H.H. and H.G. analyzed the data, and wrote the paper. X.Y. discussed the data.

The author responsible for distribution of materials integral to the findings presented in this article in accordance with the policy described in the Instructions for Authors (<https://academic.oup.com/plphys/pages/General-Instructions>) is Honghong Hu (huhh@mail.hzau.edu.cn).

## Abstract

The mechanical properties of guard cell (GC) walls are important for stomatal development and stomatal response to external stimuli. However, the molecular mechanisms of pectin synthesis and pectin composition controlling stomatal development and dynamics remain poorly explored. Here, we characterized the role of two *Arabidopsis thaliana* galacturonosyltransferases, GAUT10 and GAUT11, in plant growth, stomatal development, and stomatal dynamics. *GAUT10* and *GAUT11* double mutations reduced pectin synthesis and promoted homogalacturonan (HG) demethylesterification and demethylesterified HG degradation, resulting in larger stomatal complexes and smaller pore areas, increased stomatal dynamics, and enhanced drought tolerance of plants. In contrast, increased *GAUT10* or *GAUT11* expression impaired stomatal dynamics and drought sensitivity. Genetic interaction analyses together with immunolabeling analyses suggest that the methylesterified HG level is important in stomatal dynamics, and pectin abundance with the demethylesterified HG level controls stomatal dimension and stomatal size. Our results provide insight into the molecular mechanism of GC wall properties in stomatal dynamics, and highlight the role of *GAUT10* and *GAUT11* in stomatal dimension and dynamics through modulation of pectin biosynthesis and distribution in GC walls.

## Introduction

Stomata are formed by pairs of uniquely differentiated guard cells (GCs) in the epidermis, which regulate gas and water exchange between plants and the environment. Stomata undergo repeated and reversible opening and closing in response to various external environmental changes and intracellular signals. For example, darkness, elevated concentrations of CO<sub>2</sub>, drought, and abscisic acid promote stoma-

tal closure, whereas light and reduced concentrations of CO<sub>2</sub> induce stomatal opening (Webb et al., 2001; Kim et al., 2010; Kollist et al., 2014). These processes are achieved by reversible expansion and contraction of GCs, which is controlled by dynamic balance between intracellular turgor pressure and the physical resistance of the GC wall. Adequate GC wall elasticity and strength are needed to

ensure the functional demands of stomatal dynamics (Cosgrove, 2016). Thus, understanding the molecular mechanisms of synthesis, modification, deposition, and degradation of GC wall components is fundamental to exploring the relationship between GC structure and stomatal function (Rui et al., 2016, 2018; Rui and Anderson, 2016; Woelfenden et al., 2018; Yi et al., 2018).

The plant cell wall is 3D and consists of celluloses, hemicelluloses, pectins, and structural proteins, which are assembled into a rigid, flexible, and dynamically organized network (Somerville et al., 2004; Voiniciuc et al., 2018a). Pectins are the most complicated polysaccharide in dicots and nongraminaceous monocots primary cell walls, accounting for 50% of the *Arabidopsis* (*Arabidopsis thaliana*) leaf cell walls (Ridley et al., 2001; Jones et al., 2005; Vogel, 2008). Among the three major pectin polysaccharide types (homogalacturonan [HG], rhamnogalacturonans I (RG-I) and RG-II) (Mohnen, 2008; Caffall and Mohnen, 2009). HG, a linear homopolymer of  $\alpha$ -1,4-linked galacturonic acid, accounts for ~65% of pectins (Atmodjo et al., 2013). The HG backbone is synthesized in the Golgi apparatus in a highly methylesterified form by galacturonosyltransferases (GAUTs) and pectin methyltransferases, respectively, and then is secreted into the apoplast and demethylesterified in the cell wall by pectin methylesterases (PMEs) (Zablackis et al., 1995; Sterling et al., 2001; Mouille et al., 2007; Mohnen, 2008; Driouich et al., 2012; Atmodjo et al., 2013). PME inhibitors inhibit the activity of PMEs by direct binding (Jolie et al., 2010; Sénéchal et al., 2015). Pectins with blockwise demethylesterification tend to crosslink with  $\text{Ca}^{2+}$ , leading to wall stiffening and flexibility, whereas those with random demethylesterification are more susceptible to degradation by polygalacturonases (PGs) or pectate lyases (PLs), thus contributing to wall loosening (Xiao et al., 2014; Hocq et al., 2017; Rui et al., 2018).

GC walls are rich in pectins and have a profound effect on stomatal function. Pectin modification and degradation in GC walls are important in stomatal development and dynamics in response to different stimuli. HG methyltransferase *QUASIMODO2* mutation reduced cell adhesion in the cotyledon, with more detached GC pairs (Du et al., 2020). PMEs, *PME6*, and *PME34* are required for normal maintenance of pectin methylesterification in GC walls. *pme6* mutation caused impaired stomatal dynamics to elevated  $\text{CO}_2$  and drought sensitivity (Negi et al., 2013; Amsbury et al., 2016), and *pme34* showed a defect in stomatal aperture during heat stress conditions via altering PME and PG activity (Huang et al., 2017; Wu et al., 2017). PG *INVOLVED IN EXPANSION3* (*PGX3*), an endogenous wall-degrading pectinase, is essential for pore dimensions and stomatal dynamics by modulating pectin molecular mass and abundance (Rui et al., 2017). Pectin degradation, particularly in the middle lamella, can facilitate pore formation between two sister GCs during the last stomatal developmental step (Rui et al.,

2019). Polar stiffening contributed by pectins in GCs leads to more efficient stomatal response to altered turgor pressure, and loss of polar stiffening by PG treatment leads to a large decrease in pore aperture under any given pressure (Carter et al., 2017). Furthermore, treatment with arabinanase and feruloyl esterase impeded stomatal opening (Jones et al., 2003). However, the underlying molecular mechanisms of pectin modification and degradation in GC walls that modulate stomatal development and dynamics still remain poorly understood. Moreover, which pectin composition, the methylesterified HG or demethylesterified HG, plays the primary role in determination of stomatal development or stomatal dynamics is not known.

GAUTs function in cell wall pectin biosynthesis, by transferring GalA from uridine-diphosphate-GalA (UDP-GalA) onto HG acceptors (Sterling et al., 2006; Caffall et al., 2009). GAUTs with confirmed HG:GalA transferase activity, such as GAUT1:GAUT7 complex, GAUT4 and GAUT11, have been reported to function in plant cell wall pectin biosynthesis (Atmodjo et al., 2011; Amos et al., 2018; Biswal et al., 2018; Voiniciuc et al., 2018b). Other GAUTs with putative GAUT activity regulate cell wall properties in *Arabidopsis*. For example, *GAUT8* and *Irregular Xylem8* (*IRX8*)/*GAUT12* directly affect cell adhesion and cell wall integrity (Bouton et al., 2002; Leboeuf et al., 2005; Orfila et al., 2005; Peña et al., 2007; Persson et al., 2007). *GAUT10* is auxin responsive and regulates sugar-mediated root meristem maintenance (Pu et al., 2019). Pollen-expressed *GAUT13* and *GAUT14* function redundantly in pollen tube shape and growth (Wang et al., 2013), and *GAUT5*, *GAUT6*, and *GAUT7* are also required for HG synthesis in growing pollen tubes and HG deposition at the pollen tube apex (Lund et al., 2020). However, their functions in HG biosynthesis in GC walls are elusive, and whether or how pectin synthesis would affect pectin abundance and distribution in GC walls, thus influencing stomatal development and dynamics, remain unexplored.

We identified that closely related *GAUT10* and *GAUT11* are highly expressed in GCs and involved in pectin synthesis in GC walls. They function redundantly and play major roles in plant development, stomatal size and dimension, and stomatal dynamics to environmental changes.

## Results

### Identification of *GAUT10* and *GAUT11* in GCs

To determine whether pectin level or pectin abundance in GC walls influences stomatal function, we mainly focused on GAUTs that are highly expressed in GCs. There are 15 GAUT members in *Arabidopsis* (Caffall et al., 2009). Expression-level analyses in GC lineage cells from the public dataset (Winter et al., 2007) showed that *GAUT10*, *GAUT11*, *GAUT12*, *GAUT13*, and *GAUT14* were highly expressed in guard mother cells, young and mature GCs (Figure 1A).

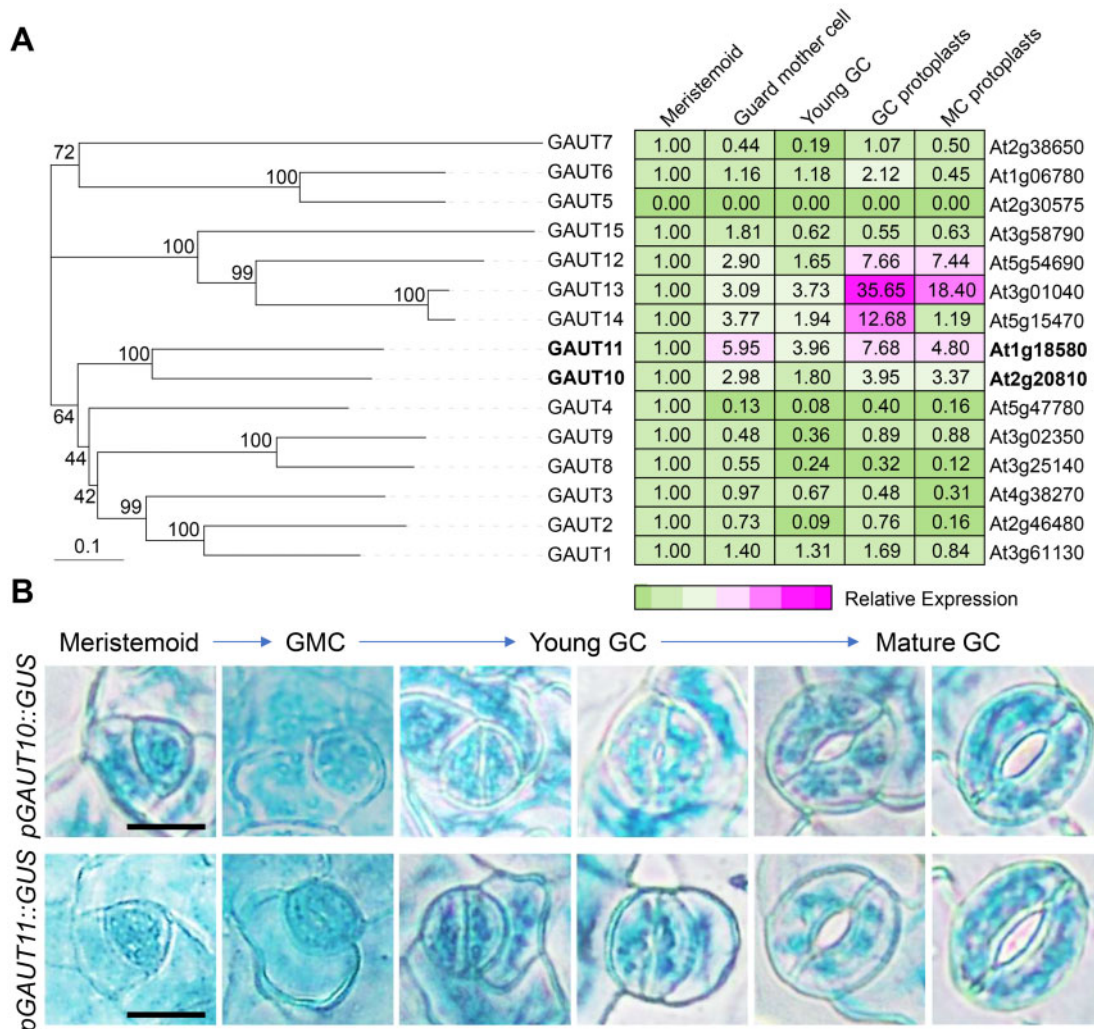


**Figure 1** Closely related homologous genes *GAUT10* and *GAUT11* are highly expressed in GCs. A, Phylogenetic analysis of GAUT proteins in Arabidopsis and relative expression of GAUTs in stomatal lineage cells based on the eFP Browser (Winter et al., 2007). Phylogenetic tree was constructed by MEGA X with the neighbor-joining method. The tree is drawn to scale, with branch lengths measured in genetic distance. For each gene, the expression level in meristemoids was set as 1.0 (green), and the expression levels in other cell types are relative to meristemoids. Different colors represent the abundance of transcripts, from low (green) to high (magenta). B, GUS staining of stomatal lineage cells at several stages of the stomatal development in *pGAUT10::GUS* and *pGAUT11::GUS* transgenic plants. Bars = 10  $\mu$ m.

GAUT12, GAUT13, and GAUT14 were reported to be involved in pollen tube growth and shape (Persson et al., 2007; Wang et al., 2013; Hao et al., 2014). We then focused on *GAUT10* and *GAUT11*, which are closely related homologous genes (Figure 1A).

To confirm that *GAUT10* and *GAUT11* are expressed in GCs, we generated transgenic plants expressing the *GUS* reporter gene controlled by the *GAUT10* or *GAUT11* promoter, respectively. *GAUT10* and *GAUT11* showed similar and broad expression patterns in embryo, cotyledons, hypocotyls, vascular strands, rosette leaves, roots, flowers, and siliques (Supplemental Figure S1A). At the cellular level, both *GAUT10* and *GAUT11* were strongly expressed in the stomatal lineage cells during GC development, including meristemoids, guard mother cells, and both young and mature GCs (Figure 1B; Supplemental Figure S1B), consistent with the

microarray data (Figure 1A). These results confirm that *GAUT10* and *GAUT11* are greatly expressed in GCs and suggest their possible involvement in stomatal biology.

### GAUT10 and GAUT11 localize in Golgi and participate in pectin synthesis

*GAUT10* and *GAUT11* belong to the glycosyltransferase family, which are considered as Golgi-localized type II membrane protein (Sterling et al., 2001, 2006; Yin et al., 2010). To determine the subcellular localizations of *GAUT10* and *GAUT11*, the *GAUT10* and *GAUT11* CDS (coding sequence) fused with a YFP tag at the C-terminus were transiently expressed in *Nicotiana benthamiana* epidermal cells. YFP fluorescence overlapped well with the Golgi-localized marker GONST1 (Baldwin et al., 2001), with punctuate distribution pattern in the transiently expressed epidermal cells and mesophyll cell

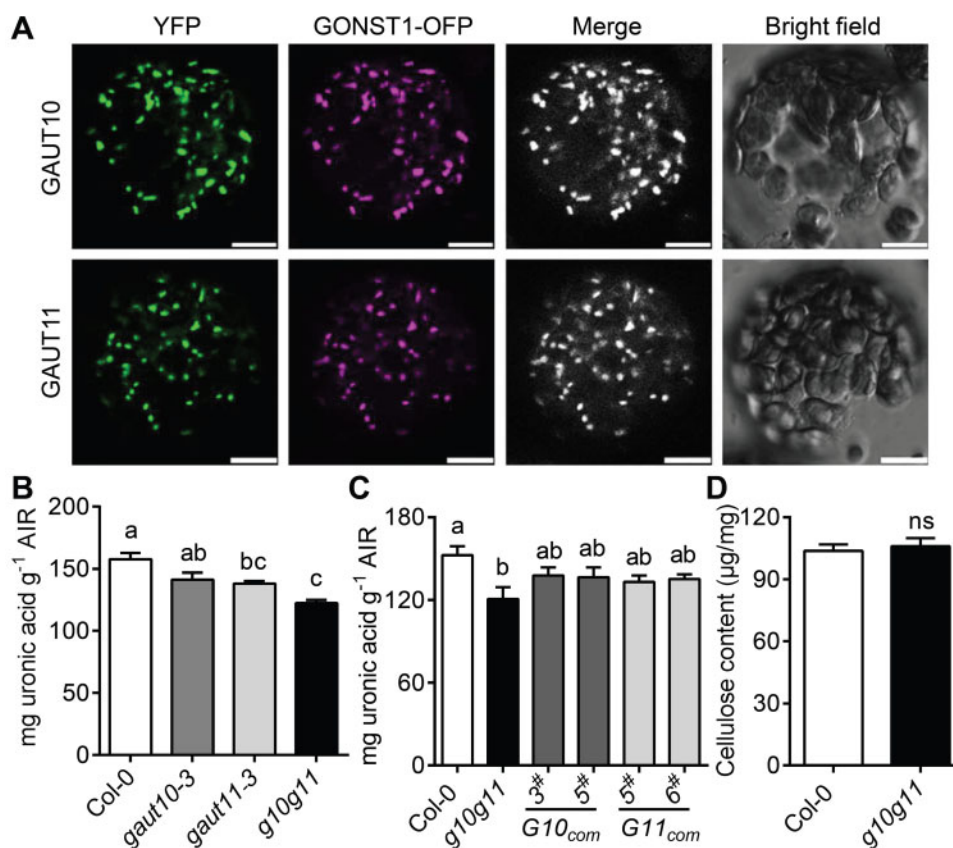


**Figure 2** GAUT10 and GAUT11 are Golgi-localized GAUTs and participate in pectin biosynthesis. A, YFP-tagged GAUT10 and GAUT11 fusion proteins are co-localized with GONST1-OPF (Golgi apparatus marker) in Golgi in MC protoplasts of *N. benthamiana* leaves. The signals were visualized with a laser confocal microscope. Bars = 10 µm. B, Uronic acid measurements in leaves from 4-week-old Col-0, *gaut10-3*, *gaut11-3*, and *g10g11* plants. Values are means ± SE (three biological replicates).  $P < 0.05$ , one-way ANOVA and Tukey's test. C, Uronic acid measurements in GAUT10 or GAUT11 complementation lines. Values are means ± SE (three biological replicates).  $P < 0.05$ , one-way ANOVA and Tukey's test. D, Cellulose content measurements by Updegraff method from leaves of 4-week-old Col-0 and *g10g11* plants. Values are means ± SE (two biological replicates). No significant difference (ns),  $P \geq 0.05$ ; Student's *t* test.

(MC) protoplasts (Figure 2A; Supplemental Figure S1C). These results confirmed that GAUT10 and GAUT11 localize to the Golgi apparatus where pectin synthesis is known to take place (Sterling et al., 2001), and are thus consistent with the possible roles of GAUT10 and GAUT11 in pectin biosynthesis.

To elucidate that GAUT10 and GAUT11 function as GAUTs in pectin biosynthesis, two T-DNA insertion mutants, *gaut10-3* (SALK\_092577) (Pu et al., 2019) and *gaut11-3* (SAIL\_567\_H05; Voinicu et al., 2018b), were ordered from the Arabidopsis Biological Resource Center (ABRC; www.arabidopsis.org; Supplemental Figure S2A). Reverse transcription-quantitative PCR (RT-qPCR) analyses revealed that *gaut10-3* was a knockout mutant, while *gaut11-3* was a knock-down mutant (Supplemental Figure S2, B and C; Supplemental Table S1). A *gaut10-3gaut11-3* (*g10g11*) double mutant was then generated and pectin content in the single and double mutant plants was determined. In this assay, alcohol-insoluble residue (AIR) was extracted from the rosette leaves and used for uronic acid content determination. *gaut11-3* exhibited a reduced total

uronic acid level compared to Col-0, consistent with a previous study (Voinicu et al., 2018b), while *gaut10-3* exhibited a uronic acid level comparable to Col-0. However, *g10g11* double mutant had much lower amount of total uronic acid level compared to Col-0 (Figure 2B). These results suggest that GAUT10 and GAUT11 function redundantly in pectin biosynthesis.

To further determine their effects on pectin synthesis, the constructs containing GAUT10 or GAUT11 genomic DNA driven by their native promoter were introduced into the *g10g11* mutants, respectively. Two independent transgenic lines expressing GAUT10 or GAUT11 (*G10<sub>com</sub>*<sup>3#</sup> and *G10<sub>com</sub>*<sup>5#</sup>, *G11<sub>com</sub>*<sup>5#</sup> and *G11<sub>com</sub>*<sup>6#</sup>), whose transcript levels were comparable or greater to that of the wild-type (WT; Supplemental Figure S2, D and E), were selected for pectin level analyses. Expression of GAUT10 or GAUT11 rescued the reduced uronic acid level of *g10g11* plants (Figure 2C), suggesting that GAUT10 and GAUT11 are functional GAUTs and involved in pectic HG synthesis. When GAUT10 or GAUT11 were overexpressed in Col-0 (*G10<sub>OE</sub>*<sup>4#</sup> and *G10<sub>OE</sub>*<sup>13#</sup>, *G11<sub>OE</sub>*<sup>7#</sup> and *G11<sub>OE</sub>*<sup>13#</sup>; Supplemental Figure S2, F and G), the

pectin levels detected by this method were not significantly increased (Supplemental Figure S3A). Because cellulose is a major cell wall structural component and is considered to be closely interacted with pectins (Broxterman and Schols, 2018), we also examined cellulose content in the *g10g11* plants by Updegraff method (Rui and Anderson, 2016). The cellulose content was not changed in the *g10g11* cell wall (Figure 2D). These results demonstrate the redundant role of *GAUT10* and *GAUT11* in pectic HG synthesis.

### GAUT10 and GAUT11 are required for plant growth and development

We determined the plant morphology of *gaut10-3*, *gaut11-3*, and *g10g11*. The *gaut10-3* and *gaut11-3* single mutants did not show any obviously altered morphologies at our growth conditions, such as plant size at both seedling and adult stages either in the half strength Murashige and Skoog (1/2 MS) medium (1% sucrose) or soil, plant height, primary root length, and seed size, compared to Col-0 (Figure 3). However, *g10g11* plants were slightly smaller than the WT at both seedling and adult stages,

with no substantial difference in plant growth rate, plant height, and leaf number compared to Col-0 (Figure 3A; Supplemental Figure S4, A and B). *g10g11* had slightly shorter primary root length at normal growth conditions and shorter hypocotyl length in darkness, the flowering time was similar to Col-0 but the fertility was severely impaired (Figure 3, B–E), suggesting *GAUT10* and *GAUT11* mutations inhibit plant growth. Furthermore, the seed size and seed germination rate of *g10g11* were substantially reduced (Figure 3F; Supplemental Figure S4C), and Ruthenium Red staining analyses showed both soluble mucilage and adherent mucilage were almost undetectable in the *g10g11* seeds, compared to the reduced mucilage levels observed in the *gaut10-3* and *gaut11-3* single mutants (Figure 3G), further supporting the functional redundancy between *GAUT10* and *GAUT11* in pectin synthesis. Additionally, when the expanded leaves were bending down 180°, around 80% of leaf petioles or midribs were broken in the *g10g11* double mutant, however, these were almost intact in Col-0 (Figure 3H). These results suggest the essential role of *GAUT10* and *GAUT11*

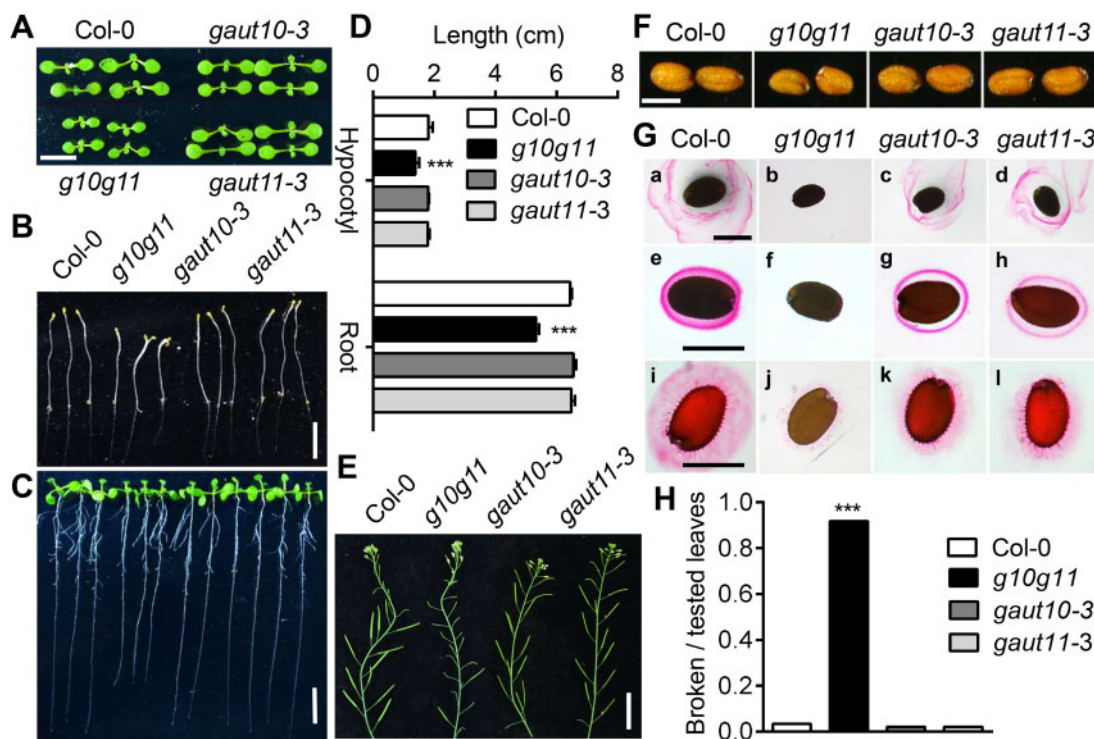


**Figure 3** *GAUT10* and *GAUT11* function in plant development. A, Eight-day-old seedlings of Col-0, *gaut10-3*, *gaut11-3*, and *g10g11*. Bar = 5 mm. B, Etiolated *g10g11* seedlings (6-d-old) exhibited shorter hypocotyls. Bar = 1 cm. C, Light-grown *g10g11* seedlings (9-d-old) exhibited shorter primary root length. Bar = 1 cm. D, Statistical analyses of hypocotyl and primary root length in (B) and (C). Values are means  $\pm$  SE ( $n \geq 30$  seedlings per genotype per experiment). Three independent experiments; \*\*\* $P < 0.001$  compared to Col-0, Student's *t* test. E, *g10g11* plants exhibited reduced fertility compared to Col-0 plants. Bar = 2 cm. F, Mature seeds of Col-0, *gaut10-3*, *gaut11-3*, and *g10g11* plants. Bars = 200  $\mu$ m. G, Ruthenium red staining of mucilage surrounding the seeds of Col-0, *gaut10-3*, *gaut11-3*, and *g10g11*. Seeds were stained directly ([a] to [d]) or after imbibition for 1 h in water ([e] to [h]) or EDTA ([i] to [l]). Bars = 200  $\mu$ m. H, Statistical analyses of broken petioles for brittleness of *g10g11* mutant leaves. Fully expanded leaves of 4- to 5-week-old plants were bent by 180° so that the adaxial surface of the leaf was parallel with the soil. Broken leaf petioles were considered brittle. Values are means  $\pm$  SE ( $n \geq 30$ , \*\*\* $P < 0.001$  compared to Col-0, Student's *t* test).

in plant growth, and the growth inhibition in *g10g11* plants may be due to the reduced pectin level, which changes the cell wall expansion and flexibility.

### GAUT10 and GAUT11 mutations result in a larger stomatal complex and smaller pore area

GAUT10 and GAUT11 are highly expressed in the stomatal lineage cells (Figure 1; Supplemental Figure S1B), we then assessed the role of GAUT10 and GAUT11 in stomata. No significant differences in stomatal density and index were found in mature *g10g11* leaves under normal growth conditions (Supplemental Figure S4, D and E). However, *g10g11* mutant plants exhibited a larger stomatal complex size in both mature leaves and cotyledons (Figure 4A; Supplemental Tables S2 and S3). In particular, the stomatal pore length and the ratio of pore length to stomatal complex length, as well as stomatal complex length and GC width, were all significantly greater in *g10g11* than in Col-0 controls (Figure 4B). In addition, *g10g11* exhibited a reduced pore width under normal conditions, resulting in smaller pore area and reduced transpiration rate (Figure 4, B–D). Consistent with these phenotypes, leaf temperature of *g10g11* plants was higher than Col-0 controls (Figure 4, E

and F). These phenotypes were all recovered to the WT level in the GAUT10 or GAUT11 complementation lines (Figure 4; Supplemental Table S2). However, in the GAUT10- or GAUT11-overexpression lines, stomatal size, and dimension did not differ from that of Col-0 (Supplemental Table S4). These results suggest that GAUT10 and GAUT11 influence GC size and stomatal pore dimension.

### Changes in GAUT10 and GAUT11 expression alter stomatal dynamics to environmental changes

We next determined the stomatal conductance changes in intact leaves of 3- to 4-week-old WT and *g10g11* mutant plants in response to changes in light intensity and CO<sub>2</sub> concentrations. Light and reduced [CO<sub>2</sub>] treatments promoted stomatal opening and thus increased stomatal conductance, and further shifts to darkness and elevated [CO<sub>2</sub>] facilitate stomatal closing in the Col-0 controls (Figure 5, A and B; Supplemental Figure S5, A and B). In contrast, the increases of stomatal conductance during light and reduced [CO<sub>2</sub>] treatments were greater in the *g10g11* mutant plants, and further stomatal closure induced by darkness and high [CO<sub>2</sub>], respectively, in *g10g11* was also faster (Figure 5, A and B; Figure S5, A–D). These results suggest that *g10g11*

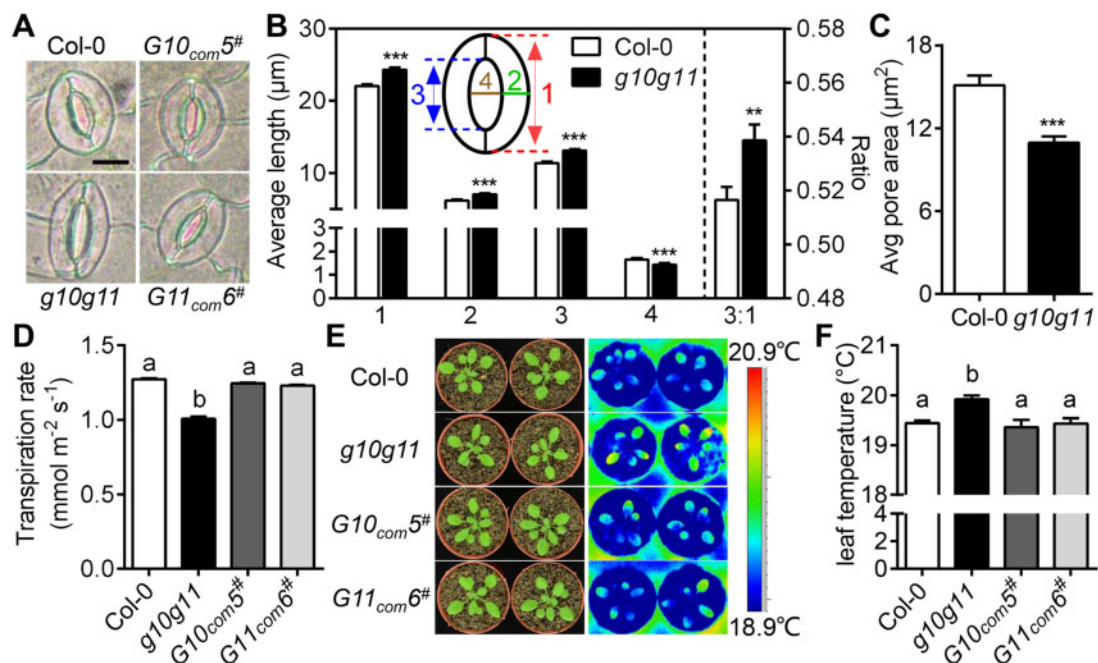


**Figure 4** GAUT10 and GAUT11 control stomatal size and pore dimension. A, Stomata in 3- to 4-week-old Col-0, *g10g11*, *G10<sub>com5</sub>#*, and *G11<sub>com6</sub>#* plants. Bars = 10 μm. B, Measurements of stomatal complex length (1), GC width (2), pore length (3), pore width (4), and the ratio of pore length to stomatal complex length (3:1) in 3- to 4-week-old Col-0 and *g10g11* plants. Values are means ± SE ( $n \geq 60$  stomata from at least six plants per genotype, \*\*\* $P < 0.001$ ; \*\* $P < 0.01$ ; Student's  $t$  test). C, Measurements of stomatal pore area in 3- to 4-week-old Col-0 and *g10g11* plants under normal growth conditions. Values are means ± SE ( $n \geq 50$  stomata from at least six plants per genotype, \*\*\* $P < 0.001$ ; Student's  $t$  test). D, Measurements of leaf transpiration rate (mmol m<sup>-2</sup> s<sup>-1</sup>) using a LI-6400XT gas exchange system in 3- to 4-week-old Col-0 and *g10g11* plants. Values are means ± SE,  $P < 0.05$ , one-way ANOVA, and Tukey's test. E, Thermal imaging of well-watered Col-0, *g10g11*, *G10<sub>com5</sub>#*, and *G11<sub>com6</sub>#* plants. F, Statistical analysis of leaf temperature from thermal images of Col-0, *g10g11*, *G10<sub>com5</sub>#*, and *G11<sub>com6</sub>#* plants. Error bars indicate ± SE,  $n \geq 6$ ,  $P < 0.05$ , one-way ANOVA, and Tukey's test.

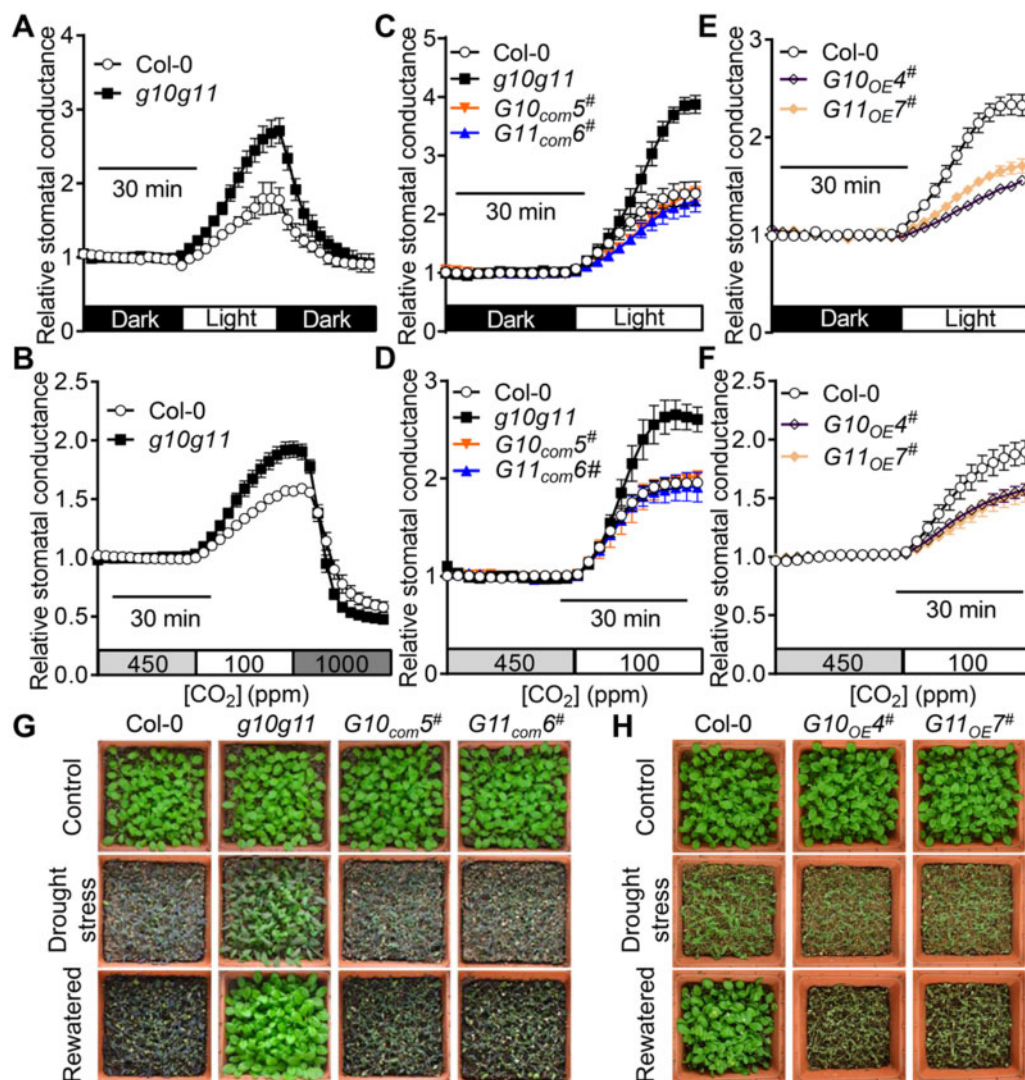


**Figure 5** *GAUT10* and *GAUT11* are involved in stomatal dynamics and drought performance. A and B, Relative stomatal conductance of 3- to 4-week-old Col-0 and *g10g11* mutant in response to shifts in light intensity or CO<sub>2</sub> concentrations. Values are means  $\pm$  SE,  $n \geq 3$  leaves per genotype per experiment. Experiments are repeated 3 times. C–F, Relative stomatal conductance of 3- to 4-week-old Col-0, *g10g11*, *G10<sub>com</sub>5<sup>#</sup>*, *G11<sub>com</sub>6<sup>#</sup>*, *G10<sub>OE</sub>4<sup>#</sup>*, and *G11<sub>OE</sub>7<sup>#</sup>* plants in response to shifts in light intensity or CO<sub>2</sub> concentrations. Values are means  $\pm$  SE,  $n \geq 3$  leaves per genotype per experiment. Experiments are repeated 3 times. G and H, Drought performance of 3-week-old Col-0, *g10g11*, *G10<sub>com</sub>5<sup>#</sup>*, *G11<sub>com</sub>6<sup>#</sup>*, *G10<sub>OE</sub>4<sup>#</sup>*, and *G11<sub>OE</sub>7<sup>#</sup>* plants under drought stresses and water recovery. Images were obtained before drought (top), drought stress for 10 d (middle) in (G) and 8 d in (H), and 2 d after re-watering (bottom).

stomata are more sensitive and have a larger range of motions in response to environmental changes in [CO<sub>2</sub>] shifts, and dark to light transitions. *G10<sub>com</sub>3<sup>#</sup>*, *G10<sub>com</sub>5<sup>#</sup>*, *G11<sub>com</sub>5<sup>#</sup>*, and *G11<sub>com</sub>6<sup>#</sup>* complementation lines behaved similar to WT with respect to stomatal dynamics to these environmental changes (Figure 5, C and D; Supplemental Figure S5, E and F), suggesting that *GAUT10* and *GAUT11* mutations cause the *g10g11* stomatal hypersensitivity. To further test whether altered stomatal dynamics in the *g10g11* mature leaves was due to the changes in stomatal dimension, we measured stomatal dynamics in the *GAUT10*- and *GAUT11*-overexpression lines, in which stomatal size and dimension were not significantly different from that in Col-0 (Supplemental Table S4). Interestingly, *G10<sub>OE</sub>4<sup>#</sup>*, *G10<sub>OE</sub>13<sup>#</sup>*,

*G11<sub>OE</sub>7<sup>#</sup>*, and *G11<sub>OE</sub>13<sup>#</sup>*-overexpression lines showed greatly impaired stomatal dynamic response to [CO<sub>2</sub>] shifts and dark to light transitions (Figure 5, E and F; Supplemental Figure S5, G and H), suggesting that the stomatal dynamics correspond with *GAUT10* and *GAUT11* expression, but not with stomatal dimension changes.

Because *g10g11* displayed reduced transpiration rate and increased stomatal response to environmental stimuli, we then performed drought stress assays of *g10g11*, and *GAUT10* or *GAUT11* complementation and overexpression lines. *g10g11* double mutant plants showed enhanced drought tolerance during exposure to drought stresses and water recovery (Figure 5G), matching well with the reduced stomatal pore area and increased stomatal dynamics

(Figures 4C and 5, A and B). *GAUT10* or *GAUT11* expression rescued the drought insensitive phenotypes (Figure 5G), and *GAUT10* or *GAUT11* overexpression lines were more sensitive to drought stresses (Figure 5H). These results suggest that *GAUT10* and *GAUT11* are essential for stomatal behavior and drought performance. These results also suggest that pectin synthesis by *GAUT10* and *GAUT11* modulates stomatal dynamics. The reduced pectin level might accelerate cell wall expansion during stomatal opening, whereas excess pectin level limits cell wall expansion.

### **GAUT10 and GAUT11 modulate HG demethylesterification and demethylesterified HG abundance in GCs**

GC pectin methylesterification status affects GC wall stiffness and stomatal dynamics (Amsbury et al., 2016). To explore whether reduced pectin synthesis changes the pectin methylesterification degree in the *g10g11* cell walls, we measured total PME activity in the leaves of 3- to 4-week-old Col-0, *g10g11*, and *GAUT10* or *GAUT11* complementation plants. *g10g11* mutant plants exhibited greater PME activity

than Col-0, while *GAUT10* or *GAUT11* complementation lines exhibited comparable PME activity as Col-0 (Figure 6A). These results suggest that *GAUT10* and *GAUT11* mutations increase pectin demethylesterification. To further determine that *GAUT10* and *GAUT11* function in GC walls, we performed immunohistochemical assays using specific antibodies that recognize different HG forms in GC walls of Col-0, *g10g11*, *G10<sub>com5</sub><sup>#</sup>*, and *G11<sub>com6</sub><sup>#</sup>* plants. Calcofluor White staining, which binds to beta-1,3 and beta-1,4 glucan chains, showed that cell wall thickness and structure were not changed in *g10g11* (Figure 6, B and C). LM19 and LM20 recognize demethylesterified HG and highly methylesterified HG, respectively. The WT GC walls were rich in demethylesterified pectins indicated by LM19 binding, and had much lower amount of methylesterified HG indicated by LM20 binding (Figure 6, B–D). Interestingly, in contrast, the immunolabeling pattern was altered in *g10g11* GC walls, in which LM19 binding was much weaker and LM20 binding was brighter than in Col-0 (Supplemental Figure 6, B–D). Moreover, *G10<sub>com5</sub><sup>#</sup>* and *G11<sub>com6</sub><sup>#</sup>* exhibited WT-like pectin distribution patterns (Figure 6, B–D). Control sections that were only incubated with secondary antibodies (without

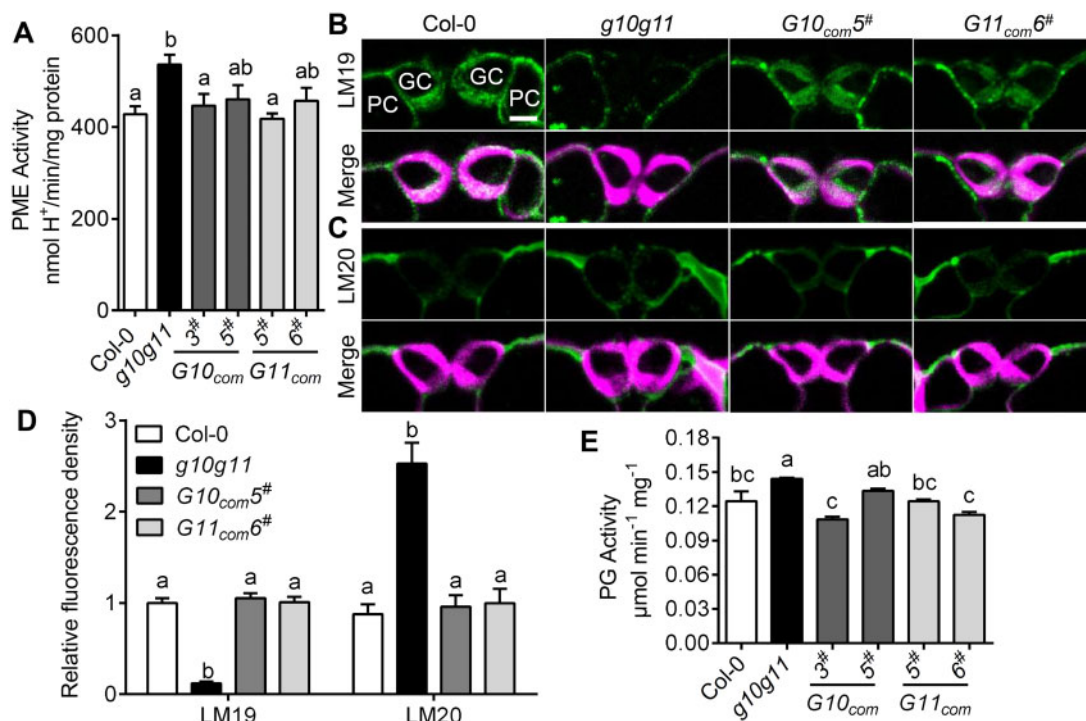


**Figure 6** *GAUT10* and *GAUT11* modulate pectin demethylesterification and abundance in GC walls. A, PME activity in the leaves of 4-week-old Col-0, *g10g11*, *G10<sub>com3</sub><sup>#</sup>*, *G10<sub>com5</sub><sup>#</sup>*, *G11<sub>com5</sub><sup>#</sup>*, and *G11<sub>com6</sub><sup>#</sup>* plants. Values are means  $\pm$  SE, three biological replicates;  $P < 0.05$ , one-way ANOVA, and Tukey's test. B, Immunolabeling of demethylesterified HG (labeled with LM19) of GC walls from WT, *g10g11*, *G10<sub>com5</sub><sup>#</sup>*, and *G11<sub>com6</sub><sup>#</sup>* plants visualized by a confocal microscope. Top panels, LM19 labeling; bottom panels, LM19 labeling (green) merged with Calcofluor White signal (magenta). PC, pavement cell. Bars = 5  $\mu$ m. C, Immunolabeling of highly methylesterified HG (labeled with LM20) of GC walls from WT, *g10g11*, *G10<sub>com5</sub><sup>#</sup>*, and *G11<sub>com6</sub><sup>#</sup>* plants. (Top), LM20 labeling; bottom, LM20 labeling (green) merged with Calcofluor White signal (magenta). Bars = 5  $\mu$ m. D, LM19 and LM20 immunolabeling fluorescence intensity in the GC walls of 3- to 4-week-old Col-0, *g10g11*, *G10<sub>com5</sub><sup>#</sup>*, and *G11<sub>com6</sub><sup>#</sup>* plants. Values are means  $\pm$  SE and letters represent significant difference ( $n \geq 20$  GCs per genotype;  $P < 0.05$ , one-way ANOVA and Tukey's test). E, PG activity in the leaves of 4-week-old Col-0, *g10g11*, *G10<sub>com3</sub><sup>#</sup>*, *G10<sub>com5</sub><sup>#</sup>*, *G11<sub>com5</sub><sup>#</sup>*, and *G11<sub>com6</sub><sup>#</sup>* plants. Values are means  $\pm$  SE, three biological replicates;  $P < 0.05$ , one-way ANOVA, and Tukey's test.



primary antibodies) showed a very low level of fluorescence in the green channel (Supplemental Figure S6). These results suggest that *GAUT10* and *GAUT11* mutations alter the pectin methylesterification degree in GC walls.

Demethylesterified HG can be degraded by HG-degrading enzyme PGs (Xiao et al., 2014; Rui et al., 2017). The very reduced demethylesterified HG in *g10g11* GC walls (Figure 6B) may be resulted from the reduced HG synthesis, or also the contribution of demethylesterified HG degradation. We then measured PG activity in *g10g11*. Surprisingly, the total PG activity was significantly increased in *g10g11* and its level was recovered to the WT-like level in *GAUT10* or *GAUT11* complementation lines (Figure 6E). These results indicate that demethylesterified HG degradation contributes to the extremely reduced demethylesterified HG level in *g10g11*. Demethylesterified HG degradation together with the reduced HG level might lead to efficient binding of LM20 on highly methylesterified HG and brighter LM20 fluorescence in *g10g11* than Col-0 (Figure 6, B and C). Similar phenomena were observed in the *PGX3* overexpression plants (Rui et al., 2017). These results suggest that *GAUT10* and *GAUT11* modulate not only pectin biosynthesis, but also HG demethylesterification and degradation in GC walls, providing molecular evidence for the altered stomatal dynamics in the *g10g11* mutant.

### PME6 mutation rescues the increased stomatal dynamics in *g10g11*

*PME6* and *PME34* are vital PMEs that are highly expressed in GCs and crucial for stomatal movement (Amsbury et al., 2016; Huang et al., 2017). We, therefore, examined *PME6* and *PME34* expression in Col-0, *g10g11*, and *GAUT10* or *GAUT11* complementation lines. RT-qPCR analyses showed that *PME6* expression was significantly greater in *g10g11*, and recovered to a similar level as Col-0 in the *GAUT10* or *GAUT11* complementation lines (Figure 7A). However, *PME34* expression was not altered in *g10g11* (Supplemental Figure S7A). These results suggest that *PME6* upregulation may be a cause for the increased PME activity and stomatal dynamics in *g10g11*.

To prove this, we generated a new *pme6* allele, *pme6-c*, using a CRISPR-Cas9 system (Ma et al., 2015). *pme6-c* had a 648-bp deletion in the *PME6* genomic DNA, which prevented normal *PME6* translation (Supplemental Figure S8, A and B). Immunolabeling assays showed that *pme6-c* had a reduced level of demethylesterified pectin indicated by LM19 binding and a greater level of highly methylesterified pectin by LM20 binding compared with Col-0 (Figure 7, B–D), consistent with a previous study (Amsbury et al., 2016). The methylesterified and demethylesterified pectin levels in *g10g11* were less than those in *pme6-c* (Figure 7, B–D), in accordance with the reduced pectin synthesis in *g10g11* (Figure 2B). The demethylesterified HG was still extremely reduced in *g10g11pme6-c* GC walls, similar to *g10g11*. However, a strong distribution of highly methylesterified pectins was observed in *g10g11pme6-c* GC walls, more than that in *pme6-c* (Figure 7, B–D),

suggesting that *PME6* mutation increases the methylesterified HG level in *g10g11* GC walls.

Interestingly, *PME6* mutation complemented the increased stomatal dynamic response in *g10g11* to CO<sub>2</sub> changes, as well as dark to light transition (Figure 7, E and F; Supplemental Figure S9, A and B). Because *GAUT10* and *GAUT11* mutations altered the stomatal dimension and size, we also observed stomatal morphology in *g10g11pme6-c* plants. *g10g11pme6-c* plants had a stomatal complex size similar to *g10g11* (Supplemental Table S5), in agreement with a previous study that *pme6* mutation did not alter the stomatal dimension (Amsbury et al., 2016). These results suggest that *PME6* upregulation is the main cause for the increased stomatal dynamics in *g10g11*, but not a major contribution for stomatal size and dimension. These findings demonstrate that *GAUT10* and *GAUT11* control GC wall flexibility, at least partially, through *PME6* modulation on pectin methylesterification to mediate stomatal dynamics.

### *PGX3* mutation cannot restore stomatal dimension and dynamics in *g10g11*

*PME6* mutation rescued *g10g11* stomatal dynamics, but not the stomatal size and dimension (Figure 7; Supplemental Table S5), and *g10g11* exhibited greater PG activity (Figure 6E), indicating that increased PG activity and demethylesterified pectin degradation may contribute to stomatal size and dimension changes. To determine which enzyme contributes to the increased PG activity, we first analyzed several PG genes that were reported to regulate plant growth and development. RT-qPCR analyses showed that the expression levels of *PGX2*, *PGX3*, *ADPG2*, and *QRT2* genes were increased in *g10g11* (Figure 8A; Supplemental Figure S7B), indicating that upregulation of these PGs could be partially responsible for the increased PG activity in *g10g11*, which may degrade the demethylesterified HG in *g10g11* GC walls. *PGX3* modulates stomatal pore dimensions and stomatal dynamics, whose overexpression led to a larger stomatal size in cotyledons and accelerated stomatal opening (Rui et al., 2017), similar to *g10g11* (Figures 4 and 5). We then generated a *PGX3* mutation by a CRISPR-Cas9 system in the *g10g11* background (Wang et al., 2015), in which 460 bp was deleted in the *PGX3* genomic DNA, resulting in a mutated form of *PGX3* (Supplemental Figure S8, A and B). The phenotypic characterization of the isolated *pgx3-c* mutant by crossing with Col-0 showed that the mutated *PGX3* gene was dysfunctional, in which stomatal dimension in cotyledons was reduced and cotyledon shape was changed (Supplemental Figure S10), consistent with a previous study (Rui et al., 2017). Immunolabeling assays showed that *PGX3* mutation slightly increased LM19 fluorescence in the *g10g11* GC walls (Figure 8, B–D), demonstrating that *PGX3* upregulation contributes to demethylesterified HG degradation and extremely reduced demethylesterified HG level in *g10g11* GC walls. However, the *g10g11pgx3-c* triple mutant showed comparable [CO<sub>2</sub>] or light-induced stomatal opening compared with *g10g11* (Figure 8, E and F; Supplemental Figure

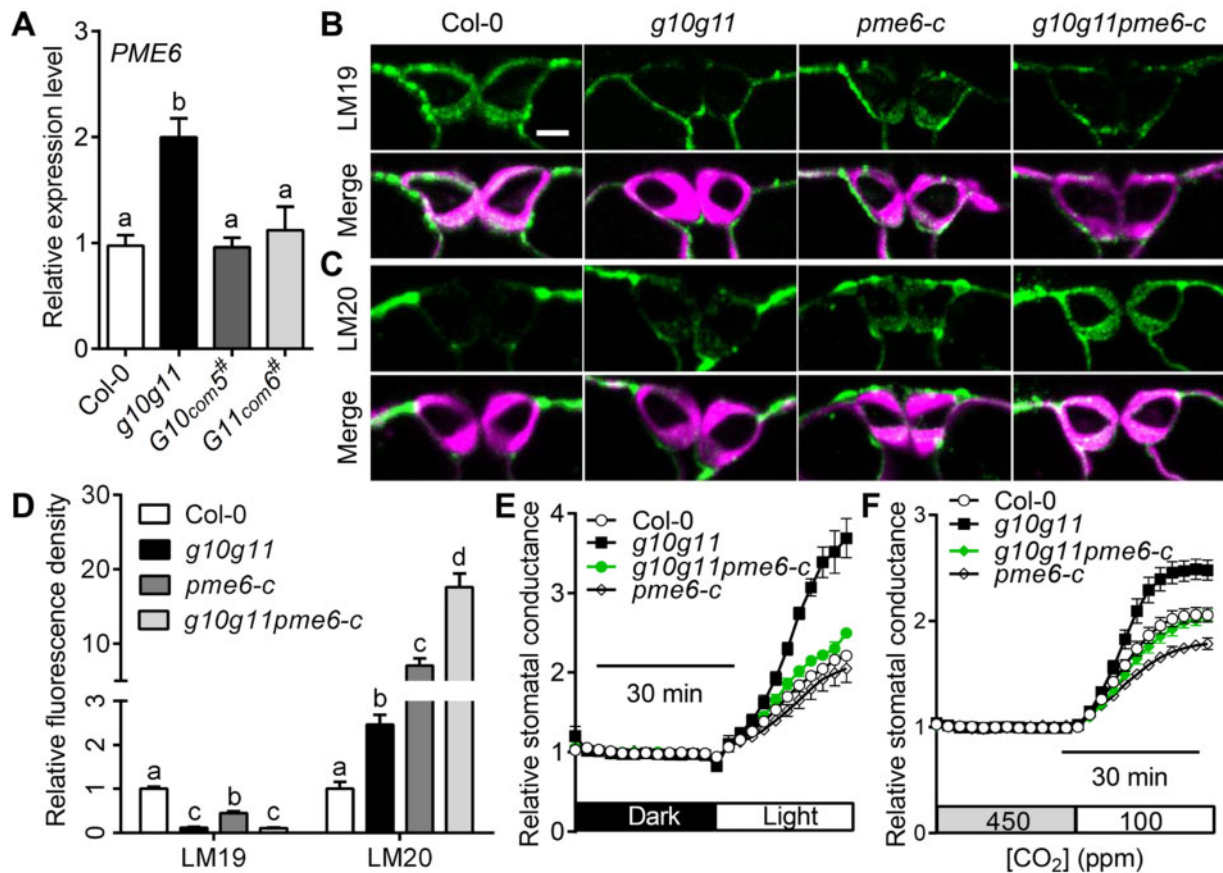


**Figure 7** *PME6* mutation rescues the stomatal hypersensitivity of *g10g11*. A, *PME6* expression level in Col-0, *g10g11*, *GAUT10*, or *GAUT11* complementation plants. Values are means  $\pm$  SE, three biological replicates;  $P < 0.05$ , one-way ANOVA, and Tukey's test. B, Immunolabeling of demethyl-esterified HG (LM19) of GC walls from Col-0, *g10g11*, *pme6-c*, and *g10g11pme6-c* plants. Top, LM19 labeling; bottom, LM19 labeling (green) merged with Calcofluor White signal (magenta). Bars = 5  $\mu$ m. C, Immunolabeling of highly methyl-esterified HG (LM20) of GC walls from Col-0, *g10g11*, *pme6-c*, and *g10g11pme6-c* plants. Top panels, LM20 labeling; bottom panels, LM20 labeling (green) merged with Calcofluor White signal (magenta). Bars = 5  $\mu$ m. D, LM19 and LM20 immunolabeling fluorescence intensity in the GC walls of 3- to 4-week-old Col-0, *g10g11*, *pme6-c*, and *g10g11pme6-c* plants. Values are means  $\pm$  SE, and letters represent significant difference ( $n \geq 20$  GCs per genotype;  $P < 0.05$ , one-way ANOVA and Tukey's test). E and F, Relative stomatal conductance in 3- to 4-week-old Col-0 controls, *g10g11*, *pme6-c*, and *g10g11pme6-c* plants in response to shifts in light intensity or CO<sub>2</sub> concentrations. Experiments are repeated 3 times. Values are means  $\pm$  SE,  $n \geq 3$  leaves per genotype per experiment.

S9, C and D), suggesting that *PGX3* upregulation is not the major reason for the increased stomatal dynamics in *g10g11*. Furthermore, *g10g11pgx3-c* triple mutant exhibited a similar stomatal morphology in both mature leaves and cotyledons (Supplemental Tables S3 and S5). Since *PGX3* regulation of stomatal morphology is only in cotyledons and the total PG activity was not significantly decreased in *g10g11pgx3-c* (Supplemental Figure S11C), these results indicate that there could be other PGs or functional redundancy in PGs, such as *PGX2*, *ADPG2*, and *QRT2* identified here, which are responsible for the increased PG activity in the *g10g11* GC walls and stomatal morphology.

## Discussion

GC development involves differential cell divisions and cell wall thickening. As the major cell wall constituents, the

pectin composition determines cell wall mechanical properties, which play a crucial role in regulating cell growth and movement in various plant physiological and developmental processes. In this study, we identify that two GAUTs GAUT10 and GAUT11, are involved in GC pectin synthesis and essential for stomatal development and stomatal dynamics in Arabidopsis (Figure 9).

GAUT1-related proteins are key players in the synthesis of pectins in plant primary cell walls (Mohnen, 2008; Caffall and Mohnen, 2009). Defects in cell wall structures have been observed in several reported GAUT1-related mutants, such as *gaut13gaut14* heterozygous (Wang et al., 2013), *irx8* (Persson et al., 2007), *qua1* (Bouton et al., 2002), *gat15* (Kong et al., 2013), and *gaut5<sup>-/-</sup>gaut6<sup>-/-</sup>gaut7<sup>+/-</sup>* mutants (Lund et al., 2020), resulting in defective plant growth phenotypes. GAUT10 and GAUT11 belong to the GAUT family, and are essential for sugar-mediated root meristem maintenance

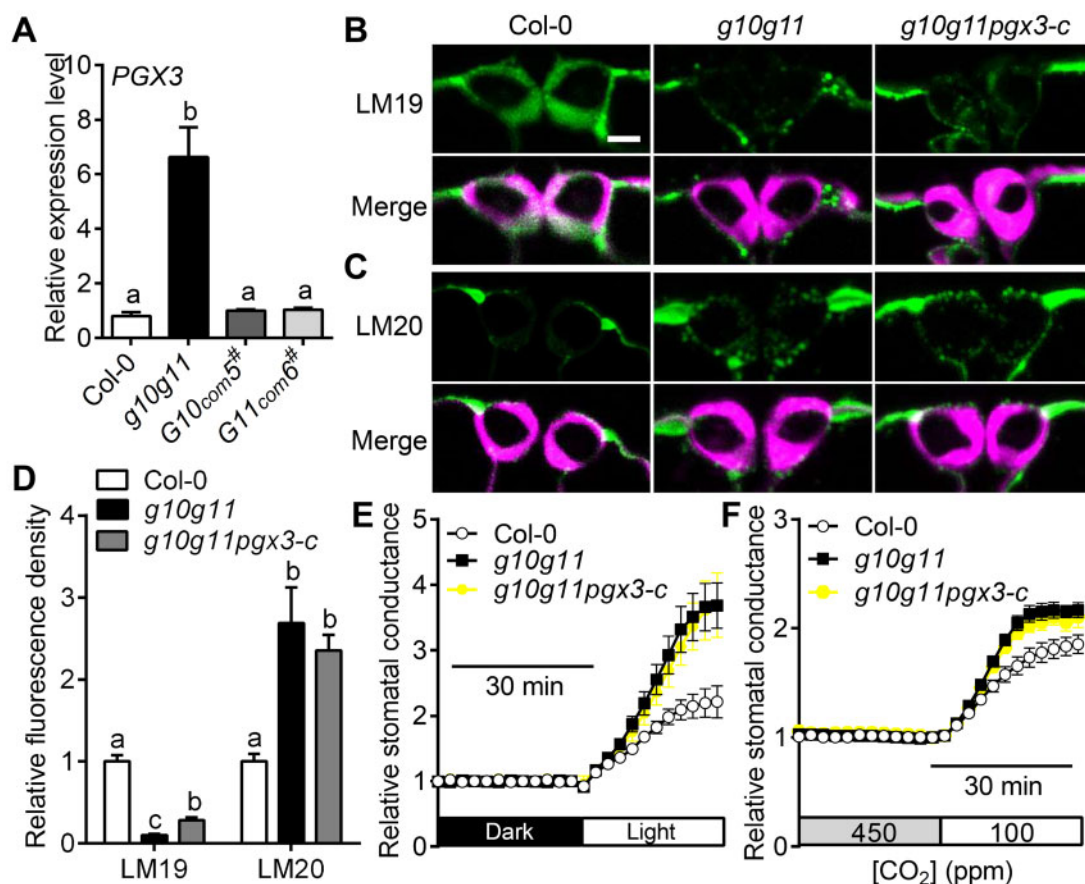


**Figure 8** PGX3 mutation cannot restore the hypersensitive stomatal dynamics of *g10g11*. A, PGX3 expression level in 3-week-old rosette leaves from Col-0, *g10g11*, *G10com5#*, and *G11com6#* plants. Values are means  $\pm$  se, three biological replicates;  $P < 0.05$ , one-way ANOVA, and Tukey's test. B, Immunolabeling of demethylesterified HG (LM19) of GC walls from Col-0, *g10g11*, and *g10g11pgx3-c* plants. Top panels, LM19 labeling; bottom panels, LM19 labeling (green) merged with Calcofluor White signal (magenta). Bars = 5  $\mu$ m. C, Immunolabeling of highly methylesterified HG (LM20) of GC walls from Col-0, *g10g11*, and *g10g11pgx3-c* plants. Top panels, LM20 labeling; bottom panels, LM20 labeling (green) merged with Calcofluor White signal (magenta). Bars = 5  $\mu$ m. D, LM19 and LM20 immunolabeling fluorescence intensity in the GC walls of 3- to 4-week-old Col-0, *g10g11*, and *g10g11pgx3-c* plants. Values are means  $\pm$  se and letters represent significant differences ( $n \geq 20$  GCs per genotype;  $P < 0.05$ , one-way ANOVA and Tukey's test). E and F, Relative stomatal conductance in 3- to 4-week-old Col-0, *g10g11* and *g10g11pgx3-c* plants in response to shifts in light intensity or CO<sub>2</sub> concentrations. Experiments are repeated 3 times. Values are means  $\pm$  se,  $n \geq 3$  leaves per genotype per experiment.

and release of seed coat mucilage (Voiniciuc et al., 2018b; Pu et al., 2019), respectively. We show that GAUT10 and GAUT11 play important roles in plant growth and development. The *g10g11* double mutant showed reduced pectin level and exhibited growth retardation, with slightly smaller plant size, shorter hypocotyl, and primary root, reduced fertility, and smaller seed size. *g10g11* also exhibited fragile leaf blades. However, no obvious growth defects were found in the *gaut10-3* and *gaut11-3* single mutants at our growth conditions (Figure 3), suggesting the functional redundancy of GAUT10 and GAUT11 in these processes. Considering that GAUT10 and GAUT11 exhibited consistent expression patterns in various tissues at different plant development stages and their involvement in pectin synthesis (Figure 2B; Supplemental Figure S1A), and the phenotypes were rescued by GAUT10 or GAUT11 expression (Figure 2C), we conclude that GAUT10 and GAUT11 have functional overlap in multiple physiological and developmental processes through

regulation of cell wall physical properties and are required for plant growth and development.

High expression of GAUT10 and GAUT11 in the stomatal lineage cells (Figure 1) indicates their involvement in pectin deposition in GC walls during stomatal development. The *g10g11* double mutant exhibited an increased stomatal dimension compared with Col-0 (Figure 4, A and B) and these phenotypes were recovered by GAUT10 or GAUT11 expression (Supplemental Table S2), suggesting that the reduced pectin level may loosen the cell wall and increase cell expansion, leading to a larger stomatal size in *g10g11* (Figure 4A). *pme6* mutation did not affect stomatal morphological phenotypes in *g10g11* (Supplemental Table S5), suggesting that the methylesterified HG level is not the main reason for the increased stomatal size and dimension. There is increasing evidence that the degradation of demethylesterified pectins by HG-degrading enzymes (e.g. PGs and PLs) and GC pressurization make contributions to pore initiation and

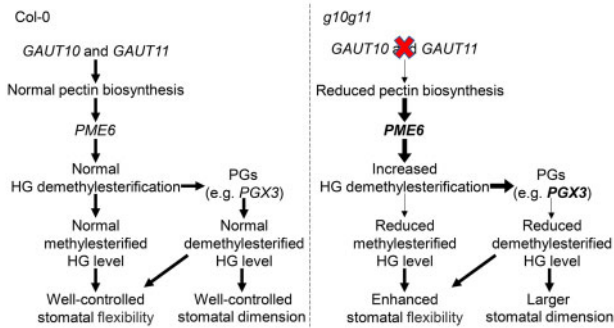


**Figure 9** Model of GAUT10 and GAUT11 in regulation of stomatal development and dynamics. Pectin is synthesized by GAUTs (GAUT10 and GAUT11) in a highly methylesterified form in Golgi apparatus and then delivered to the GC wall. Highly methylesterified HG is demethylesterified by PMEs (e.g. *PME6*), demethylesterified HG can either be cross-linked with  $\text{Ca}^{2+}$  or be degraded by PGs (e.g. *PGX3*), which coordinate to control cell wall property. In Col-0 plants, the mechanical properties of GC wall are maintained at normal levels due to the normal amounts of methylesterified and demethylesterified HG, allowing well-controlled stomatal development and dynamics. In *g10g11* mutant, reduced pectin synthesis promotes *PME6* expression and HG demethylesterification, which is in favor of PGs upregulation and PG activity on demethylesterified HG degradation, finally leading to reduced methylesterified and demethylesterified HG levels in GC walls. The reduced pectins together with the reduced demethylesterified HG level loosen the cell wall and increase cell expansion, leading to enlarged stomatal dimension and size. A reduction in pectin synthesis combined with a major contribution of reduced methylesterified HG level and minor contribution of demethylesterified HG level leads to increased stomatal flexibility. *PME6* and *PGX3* in bold mean their expressions are activated. The thick arrows indicate the processes are enhanced and the thin arrows indicate the processes are reduced.

enlargement (Rui et al., 2017, 2019). *g10g11* had increased total PME and PG activities (Figure 6, A and E), and increased expression of *PME6* and *PGs* (Supplemental Figure S7), which may contribute to the increased stomatal size and pore enlargement. Knocking out *PGX3*, whose overexpression produced a larger stomatal dimension in cotyledons as in *g10g11* (Rui et al., 2017), slightly increased demethylesterified HG level in GC wall (Figure 8, B–D), but did not restore *g10g11* stomatal morphology in either cotyledons or mature leaves (Supplemental Tables S3 and S5). Considering that the genes encoding PMEs, PGs, and PLs exist in large families (Kim et al., 2006; González-Carranza et al., 2007; McCarthy et al., 2014; Sénéchal et al., 2014) and several PG encoding genes, such as *PGX2*, *ADPG2*, and *QRT2*, were upregulated in *g10g11* (Supplemental Figure S7B), ablation of one gene might not be enough to have a significant effect on stomatal dimension in the *g10g11* background, in which the pectin level was reduced. Higher-order mutations of PGs and PLs in the *g10g11* background need to be further generated and investigated in the future. The uronic acid levels in *GAUT10*- or *GAUT11*-overexpression lines were not obviously increased in our assay, possibly because the uronic acid assays we used are not sensitive enough to detect the small increase of pectin content in the overexpressed plants,

since overexpression of *GAUT10* and *GAUT11* had opposite effect on stomatal behavior and drought performance (Figure 5). *GAUT10* or *GAUT11* overexpression may have increased pectin content in a very low amount that is not detectable by the assay we used here, and therefore enhanced the cell wall stiffness very slightly, which lead to similar stomatal size in the *GAUT10*- or *GAUT11*-overexpressing and Col-0 plants (Supplemental Table S4).

Decrease in pectin synthesis and abnormal stomatal morphology may influence stomatal behavior under various environments. *g10g11* mutants showed an increased stomatal dynamic response to external stimuli such as  $\text{CO}_2$  and light intensity changes (Figure 5, A and B; Supplemental Figure S5, A–D). Consistent with this, *g10g11* plants showed enhanced drought tolerance, whereas *GAUT10* or *GAUT11*-overexpressing plants were sensitive to drought stresses (Figure 5, G and H). The opposite stomatal behavior and drought performance correspond with *GAUT10* and *GAUT11* expression levels, suggesting the essential role of *GAUT10* and *GAUT11* and pectin abundance in stomatal dynamics. The simultaneous loss of *GAUT10* and *GAUT11* promoted HG demethylesterification and degradation, which were caused by the increased PME and PG activity and enzyme expression (Figure 6, A and E; Supplemental Figure S7). Therefore, the more flexible *g10g11* stomatal movement could be the combined result of these multiple factors. The synergistic actions of PME and PG activity are important for the maintenance of cell wall integrity, PME activity is spatially and temporally modulated in response to environmental changes, HG demethylesterification provides substrates for HG-degrading enzymes (PGs and PLs), and releases protons that promote PG activity, resulting in demethylesterified HG degradation and cell wall loosening (Moustacas et al., 1991; Hocq et al., 2017). Increased PME activity accompanied by an increased PG activity has been reported to promote pectin degradation and stomatal dynamics in both feeding assays and genetic mutants. For example, treatment with both PME and PG enzymes promoted wider stomatal opening during fusaric acid application, and reversed the impaired stomatal movement caused by arabinan degradation (Jones et al., 2003, 2005). A *pme34* mutant had greatly increased PME activity under a lethal heat-stress treatment and also an irregular increase of PG activity, which allows pectin degradation and increased stomatal opening (Huang et al., 2017; Wu et al., 2017). Similar to heat stress, reduced pectin synthesis in *g10g11* may also be a stress for plants, which produces a feedback that promotes upregulation of PMEs and random HG demethylesterification, leading to the enhanced PG activity on demethylesterified HGs degradation and GC wall loosening, thus increasing the stomatal dynamic response to environmental changes (Figure 5, A and B; Supplemental Figure S5, A–D). Further mutation of *PGX3* increased the demethylesterified HG level in *g10g11*, suggesting that PGs

act downstream of PME6 to regulate pectin modification in cell walls. Our results together with these previous findings suggest that coordination of PME and PG are important in regulating GC wall flexibility and stomatal response.

A *pme6* mutant had increased levels of highly methylesterified pectin and impaired stomatal dynamics (Amsbury et al., 2016). Knocking out *PME6* in *g10g11* not only enhanced the methylesterified HG level indicated by LM20 in GC walls, but also greatly restored the increased stomatal dynamics (Figure 7). Together with that demethylesterified HG was still absent in the GC walls of *g10g11pme6-c* (Figure 7, B–D), these results suggest that the rescue of stomatal dynamics in *g10g11pme6-c* mutant may be mainly due to the increase of highly methylesterified HG level in GC walls (Figure 7, C and D). *PGX3* overexpression showed increased stomatal dynamics (Rui et al., 2017), similar to the *g10g11* mutant (Figure 5, A and B; Supplemental Figure S5, A–D), whose mutation in *g10g11* increased demethylesterified HG level but did not recover the increased stomatal dynamics (Figure 8). These findings support the previous studies that HG demethylesterification helps increase cell wall elasticity and elevated HG methylesterification inhibits cell growth and movement (Peaucelle et al., 2011; Amsbury et al., 2016; Jonsson et al., 2021). This further suggests the key determinant role of the methylesterified HG level in regulation of stomatal dynamics at the genetic level. Our results also suggest that the increased stomatal dynamics in *g10g11* are not associated with stomatal morphological changes (Figure 5; Supplemental Tables S2 and S4). In the *GAUT10* or *GAUT11* overexpressing plants, stomatal dimension, and PME activity were not changed (Supplemental Figure S3B; Supplemental Table S4), but stomatal dynamics were impaired (Figure 5, E and F; Supplemental Figure S5, G and H). It is possible that excessive pectin can regulate the GC wall matrix and embed more pectin polymers in the cell wall frame, thus changing the cell wall properties and limiting the stomatal response to stimuli.

Mutations of *GAUT10* and *GAUT11* resulted in reduced pectin synthesis and enhanced HG demethylesterification in *g10g11* mutant plants (Figures 2, B and 6, A). Demethylesterified HG can be degraded by pectin-degrading enzymes and pectin/PLs (Xiao et al., 2014; Hocq et al., 2017; Rui et al., 2018), our experimental results showed that PG activity was increased in *g10g11* (Figure 6E). Thus the reduced pectin synthesis and degradation of demethylated pectin led to the extremely reduced demethylesterified HG level (LM19) in *g10g11* (Figure 6, B and D). *g10g11* should have reduced level of methylesterified HG in GCs; however, our immunolabeling assay showed brighter LM20 labeling (Figure 6, C and D). Similar phenomena have been reported in other studies, in which overexpression of *PGX3* also led to enhanced LM20 labeling (Rui et al., 2017), and a higher degree of HG methylesterification was observed in the *PGX1<sup>AT</sup>* cell walls (Phyo et al., 2017). The brighter LM20 labeling in *g10g11* may be caused by the extremely low level of demethylesterified HG, which lead to the highly methylesterified

HG being more accessible to LM20 for efficient labeling, or that highly methylesterified HG could not be degraded by pectin degrading enzymes. A recent report has shown that Arabidopsis PL gene *PL LIKE12* (*PLL12*) is required for normal stomatal dynamic by modulating GC wall modulus and turgor pressure and fine-tuning the levels of calcium cross-linked pectin (Chen et al., 2021). Although both PG and PL enzymes degrade demethylesterified HG, *PLL12*, and *PGX3* alter stomatal dynamics differently, and the substrate specificity between PG and PL might be different (Rui et al., 2017; Chen et al., 2021). In this study, we did not examine whether expression levels of PL genes and calcium cross-linked pectin levels were changed in the *g10g11* mutant. It is worthwhile to explore whether PL genes play a role in stomatal function of *g10g11* mutant in the future.

In conclusion, our findings identify two components that regulate HG synthesis and modulate stomatal development and dynamics, through modulation of *PME6* and *PGs* expression (Figure 9). In Col-0 plants, methylesterified and demethylesterified HG in GC walls is maintained at normal levels, which cause well-controlled stomatal development and dynamics. Mutations of *GUAT10* and *GAUT11* reduce pectin synthesis, which increases the expression levels of *PME6* and *PGs*, thus leading to the reduced methylesterified and demethylesterified HG levels in GC walls. The reduced demethylesterified HG level loosens the cell wall and increases cell expansion, leading to enlarged stomatal dimension and size. A reduction of pectin synthesis, together with reduced methylesterified and demethylesterified HG levels leads to increased stomatal flexibility. Our findings also provide insight into the mechanisms of pectin synthesis, pectin modification, and degradation in GC walls to regulate stomatal development and dynamics. Additionally, we show that the methylesterified HG is important in stomatal dynamics but not in stomatal development, such as stomatal size and dimension.

## Materials and methods

### Plant materials and growth conditions

Arabidopsis (*A. thaliana*) mutant seeds (*gaut10-3* and *gaut11-3* [Col-0 background]), were ordered from the ABRC (www.Arabidopsis.org). Surface-sterilized seeds were sown on 1/2MS plates (0.5 g/L MES, 2.2 g/L MS salts, 1% [w/v] sucrose, and 0.8% [w/v] agar, pH 5.6) or pots containing a mixture of perlite, vermiculite, and peat, and kept at 4°C in dark for 3–5 d. Plants were grown in a well-controlled growth room at 21°C with 60% relative humidity under long-day conditions (16-h light/8-h dark).

### Phylogenetic analyses and gene expression profile analyses

Arabidopsis GAUT sequences were obtained from Araport11 (Cheng et al., 2017). Alignments were performed using the MUSCLE method, and phylogenetic tree was constructed by MEGA X using the neighbor-joining method

(Kumar et al., 2018). Tree reliability was evaluated by the bootstrap method (2,500 replicates). For expression profile analyses of *GAUTs* in stomatal lineage cells, the microarray data were extracted from the eFP Browser (Winter et al., 2007). For each *GAUT*, its expression level in meristemoids was set as 1, and the heat map was constructed by TBtools (Chen et al., 2020).

### RNA isolation and gene expression analyses

Rosette leaves from 3- to 4-week-old Arabidopsis were used to isolate RNA for transcript analyses. Leaf tissues were ground to a fine powder in liquid nitrogen for total RNA extraction by Trizol reagent (Sigma, Hangzhou, China). Genomic DNA was removed by DNase I (TaKaRa, Shiga, Japan) treatment and first-strand cDNAs were synthesized from 2 µg DNase-treated RNA using the Reverse Transcription kit (Promega, Madison, WI, USA). Real-time PCR was performed using a CFX96™ Real-Time PCR Detection System (Bio-Rad, Hercules, CA, USA) according to the manufacturer's instructions. *ACTIN7* was used as an internal control.

### GUS expression and staining

The spatial expression patterns of *GAUT10* and *GAUT11* were examined by GUS expression analyses. About 2-kb fragment upstream of the start codon was used to generate the *pGAUT10::GUS* and *pGAUT11::GUS* constructs. For GUS staining, plant tissues were immersed in buffer containing 50 mM sodium phosphate, pH 7.2, 0.2% (v/v) Triton X-100, 2 mM 5-bromo-4-chloro-3-indolyl-β-D-glucuronic acid, and cyclohexylammonium salt (X-Gluc), and incubated at 37°C in the dark for 2–16 h. Tissues were decolorized in 70% ethanol for several times, and images were captured using a microscope (TS100, Nikon, Japan).

### Measurement of stomatal complex and pore size

To measure the stomatal complex size and pore dimension, abaxial epidermal layers from 3- to 4-week-old leaves were imaged by a microscope (TS100, Nikon, Japan). Stomatal pore area, stomatal pore length, GC pair height, and GC width were measured by ImageJ software. At least 60 stomata were counted.

### PME activity assay

PME activity assay was carried out according to a previous study (Richard et al., 1994). Rosette leaves of 3- to 4-week-old plants were ground to a fine powder in liquid nitrogen, then 200 µL PME extraction buffer (0.1 M citrate acid, 0.2 M Na<sub>2</sub>HPO<sub>4</sub>, and 1 M NaCl, pH 5.0) was added. The homogenate was incubated on ice for 1 h and the supernatant was collected by centrifugation at 4°C with 12,000 rpm for 15 min. Protein extracts were incubated in 1 mL of substrate solution containing 0.5% citrus pectins (Sigma-Aldrich, St Louis, MO, USA), 0.2 M NaCl, and 0.002% methyl red, pH 6.8, at 37°C for 1 h. The absorbance of the solution was measured by a spectrophotometry at 525 nm. A calibration curve was obtained by replacing the protein extracts with

5–30 µL of 0.01 M HCl to 1 mL of substrate solution. PME activity (nmol H<sup>+</sup>/min/mg protein) was calculated based on this standard curve.

### PG activity assay

Protein was extracted according to a previous study (Xiao et al., 2014). Briefly, leaf tissues were ground into a fine powder in liquid nitrogen and then mixed with extraction buffer containing 50 mM Tris-HCl (pH 7.5), 3 mM EDTA, 2.5 mM DTT, 2 mM phenylmethylsulfonyl fluoride (Sigma-Aldrich), and 1 M NaCl, and 10% (v/v) glycerol. The homogenized materials were incubated at 4°C for 1 h and the supernatant was collected by centrifugation at 20,000g and 4°C for 30 min. PG activity was measured by the increase in reducing end groups from polygalacturonic acid (poly-GalUA) (Sigma-Aldrich) by a spectrophotometer. The sample solution (50 µL) was incubated with 180 µL of 0.1% (w/v) poly-GalUA (in 40 mM sodium acetate buffer, pH 4.4) at 37°C for 10 min. The reaction was stopped by the addition of 1.2 mL of 0.1 M borate buffer (pH 9.0) and 240 µL of 1% 2-cyanoacetamide (Sigma-Aldrich) and heated at 100°C for 10 min. The solution absorbance was measured by a spectrophotometer at 276 nm (Honda et al., 1980). A blank was obtained in the same way by adding sodium acetate buffer solution instead of protein extracts. D-galacturonic acid (Sigma-Aldrich) was used as a standard.

### Preparation of AIR and uronic acid assays

Rosette leaves of 3- to 4-week-old plants were ground into a fine powder in liquid nitrogen. The powder was washed twice with 70% (v/v) ethanol and then twice with chloroform/methanol (1:1, v/v). Samples were dried by a vacuum dryer for 2 h and stored at 4°C. Uronic acid content was determined as described (Blumenkrantz and Asboe-hansen, 1973) with modifications. Briefly, samples were mixed with 1 mL concentrated sulfuric acid containing 0.0125 M sodium tetraborate (Sigma-Aldrich) and boiled for 5 min in a 100°C water bath. After cooling to room temperature, the background absorbance was read at 520 nm using a spectrophotometer. About 20 µL of 0.15% (w/v) m-hydroxydiphenyl (Sigma-Aldrich) dissolved in 0.5% (w/v) NaOH was added and incubation at room temperature for 5 min, and then the absorbance was measured at 520 nm again. A calibration curve was obtained by adding 20–100 µg/mL UDP-GalA instead of AIR.

### Cellulose content measurement

Cellulose contents were measured as described (Rui and Anderson, 2016). Rosette leaves of 3- to 4-week-old plants were incubated in 80% ethanol overnight at 65°C, and then incubated in acetone at room temperature overnight. Samples were air dried in the fume hood for 4 d and ground into powder. The powder was boiled in a solution containing acetic acid:nitric acid:water (8:2:1) for 30 min. The pellets were collected by centrifuging 12,000 rpm for 5 min and resuspended in 1 mL of 67% sulfuric acid. Fifty microliters of the resuspended samples were incubated with 1 mL of 0.2%

anthrone in concentrated sulfuric acid, the absorbance of the solution was measured by spectrophotometry at 620 nm.

### Stomatal dynamic analyses

Stomatal conductance in response to CO<sub>2</sub> concentration shifts and dark to light transitions was analyzed in intact leaves of 4-week-old plants using a portable gas-exchange system (LI-6400XT, Li-Cor) as reported (Hu et al., 2010). For plant response to CO<sub>2</sub> changes, leaves were stabilized at 450 ppm CO<sub>2</sub>, followed by 100 ppm to stimulate stomatal opening, and then shifted to 1,000 ppm to promote stomatal closure. For dark to light transitions, leaves were equilibrated at 450 ppm CO<sub>2</sub> under darkness, shifted to 150 μmol m<sup>-2</sup> s<sup>-1</sup> light intensity, and then back to darkness again.

### Immunolabeling assay

Immunolabeling assay of GC walls was performed as described (Amsbury et al., 2016). About 3- to 4-week-old leaves were trimmed into 3 mm squares and fixed in 4% paraformaldehyde. Samples were then dehydrated in an ethanol series and wrapped in resin-filled gelatin capsules (Electron Microscopy China), and polymerized for 7 d at 37°C. Sections (2-μm thick) were sliced on an ultramicrotome with a glass knife.

For immunolabeling with LM19 (PlantProbes, UK) and LM20 (PlantProbes, UK) antibodies, sections were blocked in phosphate-buffered saline solution (PBS, pH 7.2) with 3% BSA (w/v) for 1 h, and then incubated with a 1:10 dilution primary antibody in PBS buffer with 3% BSA at room temperature for 5 h. Samples were washed with PBS buffer 3 times, then incubated with anti-rat-IgG coupled to fluorescein isothiocyanate (FITC) at a 1:100 dilution in PBS buffer containing 3% BSA in the dark for 1 h, and washed again with PBS buffer 3 times. Samples were counterstained with 0.25% (w/v) Calcofluor White solution (Sigma-Aldrich) for 5 min before observation using a Leica confocal with a 488-nm excitation laser and a 520–550 nm emission filter for FITC signals and a 405 nm excitation laser and a 455 nm emission filter for Calcofluor White signals, the excitation intensity and gains set in the experiment are consistent for all samples.

### Statistics

All statistical analyses (Student's *t* test, one-way ANOVA, and Tukey's test) in this study were performed using GraphPad PRISM version 8.0 software.

### Accession numbers

Sequence data of genes covered in this article can be found in the Arabidopsis Genome Initiative or GenBank/EMBL databases under the following accession numbers: *GAUT10* (AT2G20810), *GAUT11* (AT1G18580), *PME6* (AT1G23200), and *PGX3* (AT1G48100).

### Supplemental data

The following materials are available in the online version of this article.

**Supplemental Figure S1.** Expression pattern and subcellular localization of *GAUT10* and *GAUT11*.

**Supplemental Figure S2.** Gene structure and transcript analyses of *GAUT10* and *GAUT11*.

**Supplemental Figure S3.** Total uronic acid content and PME activity are not changed in *GAUT10* or *GAUT11* overexpression lines.

**Supplemental Figure S4.** Phenotypic characterization of *g10g11* mutant.

**Supplemental Figure S5.** *GAUT10* and *GAUT11* modulate stomatal dynamics in response to light and CO<sub>2</sub> changes.

**Supplemental Figure S6.** Control images for immunolabeling in GC walls.

**Supplemental Figure S7.** Expression levels of *PME* and *PG* genes in the *g10g11* mutant.

**Supplemental Figure S8.** Schematic of gene structure and transcript analysis of *PME6* and *PGX3*.

**Supplemental Figure S9.** *PME6* mutation rescues stomatal dynamic response to CO<sub>2</sub> and light changes in *g10g11*.

**Supplemental Figure S10.** *pgx3-c* mutant showed defects in seedling development and cotyledon stomatal development.

**Supplemental Figure S11.** Mutation of *PME6* or *PGX3* does not affect the increased PME or PG activity in the *g10g11* mutant.

**Supplemental Table S1.** Primers used in this study.

**Supplemental Table S2.** Measurement of stomatal dimensions in *g10g11* and *GAUT* complementation lines.

**Supplemental Table S3.** Measurement of stomatal dimensions in cotyledons of Col-0, *g10g11*, and *g10g11pgx3-c* plants.

**Supplemental Table S4.** Measurement of stomatal dimensions in Col-0 and *GAUT* overexpression lines.

**Supplemental Table S5.** Measurement of stomatal dimensions in mature leaves of Col-0, *g10g11*, *pme6-c*, *g10g11pme6-c*, and *g10g11pgx3-c* plants.

### Acknowledgments

The authors thank Dr Zhuqing Zhou (Huazhong Agricultural University) for providing the ultramicrotome.

### Funding

This work was supported by grants from the National Natural Science Foundation (31970730, 31771552) and the National Key Research and Development Program of China (2016YFD0100606).

*Conflict of interest statement.* The authors declare no conflicts of interest.

### References

Amos RA, Pattathil S, Yang JY, Atmodjo MA, Urbanowicz BR, Moremen KW, Mohnen D (2018) A two-phase model for the non-processive biosynthesis of homogalacturonan polysaccharides by the GAUT1:GAUT7 complex. *J Biol Chem* **293**: 19047–19063

- Amsbury S, Hunt L, Elhaddad N, Baillie A, Lundgren M, Verherbruggen Y, Scheller HV, Knox JP, Fleming AJ, Gray JE (2016) Stomatal function requires pectin de-methyl-esterification of the guard cell wall. *Curr Biol* **26**: 2899–2906
- Atmodjo MA, Hao Z, Mohnen D (2013) Evolving views of pectin biosynthesis. *Annu Rev Plant Biol* **64**: 747–779
- Atmodjo MA, Sakuragi Y, Zhu X, Burrell AJ, Mohanty SS, Atwood JA, 3rd, Orlando R, Scheller HV, Mohnen D (2011) Galacturonosyltransferase (GAUT)1 and GAUT7 are the core of a plant cell wall pectin biosynthetic homogalacturonan: galacturonosyltransferase complex. *Proc Natl Acad Sci USA* **108**: 20225–20230
- Baldwin TC, Handford MG, Yuseff MI, Orellana A, Dupree P (2001) Identification and characterization of GONST1, a golgi-localized GDP-mannose transporter in Arabidopsis. *Plant Cell* **13**: 2283–2295
- Biswal AK, Atmodjo MA, Li M, Baxter HL, Yoo CG, Pu Y, Lee YC, Mazarei M, Black IM, Zhang JY, et al. (2018) Sugar release and growth of biofuel crops are improved by downregulation of pectin biosynthesis. *Nat Biotechnol* **36**: 249–257
- Blumenkrantz N, Asboe-hansen G (1973) New method for quantitative determination of uronic acids. *Anal Biochem* **54**: 484–489
- Bouton S, Leboeuf E, Mouille G, Leydecker MT, Talbotec J, Granier F, Lahaye M, Höfte H, Truong HN (2002) QUASIMODO1 encodes a putative membrane-bound glycosyltransferase required for normal pectin synthesis and cell adhesion in Arabidopsis. *Plant Cell* **14**: 2577–2590
- Broxterman SE, Schols HA (2018) Interactions between pectin and cellulose in primary plant cell walls. *Carbohydr Polym* **192**: 263–272
- Caffall KH, Mohnen D (2009) The structure, function, and biosynthesis of plant cell wall pectic polysaccharides. *Carbohydr Res* **344**: 1879–1900
- Caffall KH, Pattathil S, Phillips SE, Hahn MG, Mohnen D (2009) Arabidopsis thaliana T-DNA mutants implicate GAUT genes in the biosynthesis of pectin and xylan in cell walls and seed testa. *Mol Plant* **2**: 1000–1014
- Carter R, Woolfenden H, Baillie A, Amsbury S, Carroll S, Healicon E, Sovatzoglou S, Braybrook S, Gray JE, Hobbs J, et al. (2017) Stomatal opening involves polar, not radial, stiffening of guard cells. *Curr Biol* **27**: 2974–2983 e2972
- Chen C, Chen H, Zhang Y, Thomas HR, Frank MH, He Y, Xia R (2020) TBtools: an integrative toolkit developed for interactive analyses of big biological data. *Mol Plant* **13**: 1194–1202
- Chen Y, Li W, Turner JA, Anderson CT (2021) PECTATE LYASE LIKE12 patterns the guard cell wall to coordinate turgor pressure and wall mechanics for proper stomatal function in Arabidopsis. *Plant Cell* doi: 10.1093/plcell/koab161
- Cheng CY, Krishnakumar V, Chan AP, Thibaud-Nissen F, Schobel S, Town CD (2017) Araport11: a complete reannotation of the Arabidopsis thaliana reference genome. *Plant J* **89**: 789–804
- Cosgrove DJ (2016) Plant cell wall extensibility: connecting plant cell growth with cell wall structure, mechanics, and the action of wall-modifying enzymes. *J Exp Bot* **67**: 463–476
- Driouich A, Follet-Gueye ML, Bernard S, Kousar S, Chevalier L, Vire-Gibouin M, Lerouxel O (2012) Golgi-mediated synthesis and secretion of matrix polysaccharides of the primary cell wall of higher plants. *Front Plant Sci* **3**: 79
- Du J, Kirui A, Huang S, Wang L, Barnes WJ, Kiemle SN, Zheng Y, Rui Y, Ruan M, Qi S, et al. (2020) Mutations in the pectin methyltransferase QUASIMODO2 influence cellulose biosynthesis and wall integrity in Arabidopsis. *Plant Cell* **32**: 3576–3597
- González-Carranza ZH, Elliott KA, Roberts JA (2007) Expression of polygalacturonases and evidence to support their role during cell separation processes in Arabidopsis thaliana. *J Exp Bot* **58**: 3719–3730
- Hao Z, Avci U, Tan L, Zhu X, Glushka J, Pattathil S, Eberhard S, Sholes T, Rothstein GE, Lukowitz W, et al. (2014) Loss of Arabidopsis GAUT12/IRX8 causes anther indehiscence and leads to reduced G lignin associated with altered matrix polysaccharide deposition. *Front Plant Sci* **5**: 357
- Hocq L, Pelloux J, Lefebvre V (2017) Connecting homogalacturonan-type pectin remodeling to acid growth. *Trends Plant Sci* **22**: 20–29
- Honda S, Matsuda Y, Takahashi M, Kakehi K, Ganno S (1980) Fluorimetric determination of reducing carbohydrates with 2-cyanoacetamide and application to automated analysis of carbohydrates as borate complexes. *Anal Chem* **52**: 1079–1082
- Hu H, Boisson-Dernier A, Israelsson-Nordstrom M, Bohmer M, Xue S, Ries A, Godoski J, Kuhn JM, Schroeder JI (2010) Carbonic anhydrases are upstream regulators of CO<sub>2</sub>-controlled stomatal movements in guard cells. *Nat Cell Biol* **12**: 87–93
- Huang YC, Wu HC, Wang YD, Liu CH, Lin CC, Luo DL, Jinn TL (2017) PECTIN METHYLESTERASE34 contributes to heat tolerance through its role in promoting stomatal movement. *Plant Physiol* **174**: 748–763
- Jolie RP, Duvetter T, Van Loey AM, Hendrickx ME (2010) Pectin methylesterase and its proteinaceous inhibitor: a review. *Carbohydr Res* **345**: 2583–2595
- Jones L, Milne JL, Ashford D, McCann MC, McQueen-Mason SJ (2005) A conserved functional role of pectic polymers in stomatal guard cells from a range of plant species. *Planta* **221**: 255–264
- Jones L, Milne JL, Ashford D, McQueen-Mason SJ (2003) Cell wall arabinan is essential for guard cell function. *Proc Natl Acad Sci USA* **100**: 11783–11788
- Jonsson K, Lathe RS, Kierzkowski D, Routier-Kierzkowska AL, Hamant O, Bhalerao RP (2021) Mechanochemical feedback mediates tissue bending required for seedling emergence. *Curr Biol* **31**: 1154–1164
- Kim J, Shiu SH, Thoma S, Li WH, Patterson SE (2006) Patterns of expansion and expression divergence in the plant polygalacturonase gene family. *Genome Biol* **7**: R87
- Kim TH, Bohmer M, Hu H, Nishimura N, Schroeder JI (2010) Guard cell signal transduction network: advances in understanding abscisic acid, CO<sub>2</sub>, and Ca<sup>2+</sup> signaling. *Annu Rev Plant Biol* **61**: 561–591
- Kollist H, Nuhkat M, Roelfsema MR (2014) Closing gaps: linking elements that control stomatal movement. *New Phytol* **203**: 44–62
- Kong Y, Zhou G, Abdeen AA, Schafhauser J, Richardson B, Atmodjo MA, Jung J, Wicker L, Mohnen D, Western T, et al. (2013) GALACTURONOSYLTRANSFERASE-LIKE5 is involved in the production of Arabidopsis seed coat mucilage. *Plant Physiol* **163**: 1203–1217
- Kumar S, Stecher G, Li M, Knyaz C, Tamura K (2018) MEGA X: molecular evolutionary genetics analysis across computing platforms. *Mol Biol Evol* **35**: 1547–1549
- Leboeuf E, Guillon F, Thoiron S, Lahaye M (2005) Biochemical and immunohistochemical analysis of pectic polysaccharides in the cell walls of Arabidopsis mutant QUASIMODO 1 suspension-cultured cells: implications for cell adhesion. *J Exp Bot* **56**: 3171–3182
- Lund CH, Stenbaek A, Atmodjo MA, Rasmussen RE, Moller IE, Erstad SM, Biswal AK, Mohnen D, Mravec J, Sakuragi Y (2020) Pectin synthesis and pollen tube growth in Arabidopsis involves three GAUT1 Golgi-anchoring proteins: GAUT5, GAUT6, and GAUT7. *Front Plant Sci* **11**: 585774
- Ma X, Zhang Q, Zhu Q, Liu W, Chen Y, Qiu R, Wang B, Yang Z, Li H, Lin Y, et al. (2015) A robust CRISPR/Cas9 system for convenient, high-efficiency multiplex genome editing in monocot and dicot plants. *Mol Plant* **8**: 1274–1284
- McCarthy TW, Der JP, Honaas LA, dePamphilis CW, Anderson CT (2014) Phylogenetic analysis of pectin-related gene families in Physcomitrella patens and nine other plant species yields evolutionary insights into cell walls. *BMC Plant Biol* **14**: 79
- Mohnen D (2008) Pectin structure and biosynthesis. *Curr Opin Plant Biol* **11**: 266–277
- Mouille G, Ralet MC, Cavelier C, Eland C, Effroy D, Hematy K, McCartney L, Truong HN, Gaudon V, Thibault JF, et al. (2007)



- Homogalacturonan synthesis in *Arabidopsis thaliana* requires a Golgi-localized protein with a putative methyltransferase domain. *Plant J* **50**: 605–614
- Moustacas AM, Nari J, Borel M, Noat G, Ricard J** (1991) Pectin methylesterase, metal ions and plant cell-wall extension. The role of metal ions in plant cell-wall extension. *Biochem J* **279**: 351–354
- Negi J, Moriwaki K, Konishi M, Yokoyama R, Nakano T, Kusumi K, Hashimoto-Sugimoto M, Schroeder JI, Nishitani K, Yanagisawa S, et al.** (2013) A Dof transcription factor, SCAP1, is essential for the development of functional stomata in *Arabidopsis*. *Curr Biol* **23**: 479–484
- Orfila C, Sørensen SO, Harholt J, Geshi N, Crombie H, Truong HN, Reid JS, Knox JP, Scheller HV** (2005) QUASIMODO1 is expressed in vascular tissue of *Arabidopsis thaliana* inflorescence stems, and affects homogalacturonan and xylan biosynthesis. *Planta* **222**: 613–622
- Peaucelle A, Braybrook SA, Le Guillou L, Bron E, Kuhlemeier C, Höfte H** (2011) Pectin-induced changes in cell wall mechanics underlie organ initiation in *Arabidopsis*. *Curr Biol* **21**: 1720–1726
- Peña MJ, Zhong R, Zhou GK, Richardson EA, O'Neill MA, Davill AG, York WS, Ye ZH** (2007) *Arabidopsis* irregular xylem8 and irregular xylem9: implications for the complexity of glucuronoxylan biosynthesis. *Plant Cell* **19**: 549–563
- Persson S, Caffall KH, Freshour G, Hilley MT, Bauer S, Poindexter P, Hahn MG, Mohnen D, Somerville C** (2007) The *Arabidopsis* irregular xylem8 mutant is deficient in glucuronoxylan and homogalacturonan, which are essential for secondary cell wall integrity. *Plant Cell* **19**: 237–255
- Phyo P, Wang T, Xiao C, Anderson CT, Hong M** (2017) Effects of pectin molecular weight changes on the structure, dynamics, and polysaccharide interactions of primary cell walls of *Arabidopsis thaliana*: insights from solid-state NMR. *Biomacromolecules* **18**: 2937–2950
- Pu Y, Walley JW, Shen Z, Lang MG, Briggs SP, Estelle M, Kelley DR** (2019) Quantitative early auxin root proteomics identifies GAUT10, a galacturonosyltransferase, as a novel regulator of root meristem maintenance. *Mol Cell Proteomics* **18**: 1157–1170
- Richard L, Qin LX, Gadal P, Goldberg R** (1994) Molecular cloning and characterisation of a putative pectin methylesterase cDNA in *Arabidopsis thaliana* (L.). *FEBS Lett* **355**: 135–139
- Ridley BL, O'Neill MA, Mohnen D** (2001) Pectins: structure, biosynthesis, and oligogalacturonide-related signaling. *Phytochemistry* **57**: 929–967
- Rui Y, Anderson CT** (2016) Functional analysis of cellulose and xyloglucan in the walls of stomatal guard cells of *Arabidopsis*. *Plant Physiol* **170**: 1398–1419
- Rui Y, Chen Y, Kandemir B, Yi H, Wang JZ, Puri VM, Anderson CT** (2018) Balancing strength and flexibility: how the synthesis, organization, and modification of guard cell walls govern stomatal development and dynamics. *Front Plant Sci* **9**: 1202
- Rui Y, Chen Y, Yi H, Purzycki T, Puri VM, Anderson CT** (2019) Synergistic pectin degradation and guard cell pressurization underlie stomatal pore formation. *Plant Physiol* **180**: 66–77
- Rui Y, Xiao C, Yi H, Kandemir B, Wang JZ, Puri VM, Anderson CT** (2017) POLYGALACTURONASE INVOLVED IN EXPANSION3 functions in seedling development, rosette growth, and stomatal dynamics in *Arabidopsis thaliana*. *Plant Cell* **29**: 2413–2432
- Rui Y, Yi H, Kandemir B, Wang JZ, Puri VM, Anderson CT** (2016) Integrating cell biology, image analysis, and computational mechanical modeling to analyze the contributions of cellulose and xyloglucan to stomatal function. *Plant Signal Behav* **11**: e1183086
- Sénéchal F, L'Enfant M, Domon JM, Rosiau E, Crépeau MJ, Surcouf O, Esquivel-Rodriguez J, Marcelo P, Mareck A, Guérineau F, et al.** (2015) Tuning of pectin methylesterification: pectin methylesterase inhibitor 7 modulates the processive activity of co-expressed pectin methylesterase 3 in a pH-dependent manner. *J Biol Chem* **290**: 23320–23335
- Sénéchal F, Wattier C, Rustérucci C, Pelloux J** (2014) Homogalacturonan-modifying enzymes: structure, expression, and roles in plants. *J Exp Bot* **65**: 5125–5160
- Somerville C, Bauer S, Brininstool G, Facette M, Hamann T, Milne J, Osborne E, Paredes A, Persson S, Raab T, et al.** (2004) Toward a systems approach to understanding plant cell walls. *Science* **306**: 2206–2211
- Sterling JD, Atmodjo MA, Inwood SE, Kumar Kolli VS, Quigley HF, Hahn MG, Mohnen D** (2006) Functional identification of an *Arabidopsis* pectin biosynthetic homogalacturonan galacturonosyltransferase. *Proc Natl Acad Sci USA* **103**: 5236–5241
- Sterling JD, Quigley HF, Orellana A, Mohnen D** (2001) The catalytic site of the pectin biosynthetic enzyme alpha-1,4-galacturonosyltransferase is located in the lumen of the Golgi. *Plant Physiol* **127**: 360–371
- Vogel J** (2008) Unique aspects of the grass cell wall. *Curr Opin Plant Biol* **11**: 301–307
- Voiniciuc C, Engle KA, Günl M, Dieluweit S, Schmidt MHW, Yang JY, Moremen KW, Mohnen D, Usadel B** (2018b) Identification of key enzymes for pectin synthesis in seed mucilage. *Plant Physiol* **178**: 1045–1064
- Voiniciuc C, Pauly M, Usadel B** (2018a) Monitoring polysaccharide dynamics in the plant cell wall. *Plant Physiol* **176**: 2590–2600
- Wang L, Wang W, Wang YQ, Liu YY, Wang JX, Zhang XQ, Ye D, Chen LQ** (2013) *Arabidopsis* galacturonosyltransferase (GAUT) 13 and GAUT14 have redundant functions in pollen tube growth. *Mol Plant* **6**: 1131–1148
- Wang ZP, Xing HL, Dong L, Zhang HY, Han CY, Wang XC, Chen QJ** (2015) Egg cell-specific promoter-controlled CRISPR/Cas9 efficiently generates homozygous mutants for multiple target genes in *Arabidopsis* in a single generation. *Genome Biol* **16**: 144
- Webb AA, Larman MG, Montgomery LT, Taylor JE, Hetherington AM** (2001) The role of calcium in ABA-induced gene expression and stomatal movements. *Plant J* **26**: 351–362
- Winter D, Vinegar B, Nahal H, Ammar R, Wilson GV, Provart NJ** (2007) An "Electronic Fluorescent Pictograph" browser for exploring and analyzing large-scale biological data sets. *PLoS One* **2**: e718
- Woelfenden HC, Baillie AL, Gray JE, Hobbs JK, Morris RJ, Fleming AJ** (2018) Models and mechanisms of stomatal mechanics. *Trends Plant Sci* **23**: 822–832
- Wu HC, Huang YC, Stracovsky L, Jinn TL** (2017) Pectin methylesterase is required for guard cell function in response to heat. *Plant Signal Behav* **12**: e1338227
- Xiao C, Somerville C, Anderson CT** (2014) POLYGALACTURONASE INVOLVED IN EXPANSION1 functions in cell elongation and flower development in *Arabidopsis*. *Plant Cell* **26**: 1018–1035
- Yi H, Rui Y, Kandemir B, Wang JZ, Anderson CT, Puri VM** (2018) Mechanical effects of cellulose, xyloglucan, and pectins on stomatal guard cells of *Arabidopsis thaliana*. *Front Plant Sci* **9**: 1566
- Yin Y, Chen H, Hahn MG, Mohnen D, Xu Y** (2010) Evolution and function of the plant cell wall synthesis-related glycosyltransferase family 8. *Plant Physiol* **153**: 1729–1746
- Zablackis E, Huang J, Müller B, Davill AG, Albersheim P** (1995) Characterization of the cell-wall polysaccharides of *Arabidopsis thaliana* leaves. *Plant Physiol* **107**: 1129–1138